CRITICAL FLOW COMPUTER MODELLING USING TRACE CODE

Lappeenranta–Lahti University of Technology LUT

Master's Degree Program in Nuclear Engineering

2022

Nathan de Carvalho Braz

Examiner(s): Professor, Juhani Hyvärinen

Dr. Juhani Vihavainen

ABSTRACT

Lappeenranta–Lahti University of Technology LUT
LUT School of Energy Systems
Energy Technology

Nathan de Carvalho Braz

Critical Flow Computer Modelling Using Trace Code

Master's thesis
2022
82 pages, 76 figures, 3 tables

Examiner(s): Professor, Juhani Hyvärinen and Dr. Juhani Vihavainen

Keywords: Critical Flow, Void fraction, Trace Code, Safety, Nuclear Power Plant.

In this paper critical flow and void fraction will be observed as a result of simulation comparing several initial data. Concerns about safety in nuclear energy industries has become number one priority after several nuclear accidents over the years since nuclear fissions has become one of the sources for energy around the globe. The world is so worry about how safe a nuclear power plant is and with that over 60 power plants has been shut down. As severe accident caused by leaking on internal pipes tubes of a operant power plant or even by other types of leaking in other parts insight a power plant has to be study. In this work it's possible to understand of how an operating power plant works, understand its pieces so it can be clear the work done about the pipes insight a steam generator.

ACKNOWLEDGEMENTS

To begin I would like to thank the LUT School of Energy for this opportunity and explore and share all this knowledge that I will carry with me for the rest of my life, not only insight the classes but outside.

Also, big thank to my supervisor Dr Juhani Vihavainen for the patient, education, guide and understanding that life not always is the way we have planned and sometimes there are stones on the way, but we can cross it.

Further I want to thank my mom Ellen to support me in this journey, to always be by my side and always be there, the friends that were with me in this journey in special Orlando, the friends in Russia and all around the world that I have met during my life and education for also be by my side.

Finally, I want to thank my family, friend of my hometown and my grandmother that unfortunately has passed away during this education but I know that she is in a best place now and rutting for me.

A big thank to you all.

Lappeenranta, 25.11.2022

Nathan de Carvalho Braz

SYMBOLS AND ABBREVIATIONS

d	diameter	[m2]
h	height	[m]
p	pressure	[bar, Pa]
T	temperature	[oC, K]
t	time	[s]
Δm	mass flow	[kg/s]

Greek characters

ρ	density

Subscripts

0	start time
conv	conversion
core	reactor core
evap	evaporation
hyd	hydraulic sat saturation

Abbreviations

BWR – Boiling Water Reactor

CP – Primary Pump

CRD – Control Rod Drive

EPR – European Pressurised Water Reactor

ESBWR – Economic Simplified Boiling Water Reactor FMCRD – Fine Motion Control Rod Drive

FW – Feedwater

IAEA – International Atomic Energy Agency

LOCA - Loss Of Coolant Accidents

LUT – Lappeenranta-Lahti University of Technology

NRC – Nuclear Regulatory Commission

NPP – Nuclear Power Plant

NR – Nuclear Reactor

OECD - Organization for Economic Cooperation and Development

P – Pressurizor

PWR – Power Water Reactor

PCCS – Passive Containment Cooling System

PCV – Primary Containment Vessel

RCS – Reactor Coolant System

RPV – Reactor Pressure vessel

RPS – Reactor Protection System

SG – Steam Generator

STUK - Finland Nuclear Safety Authority

THS - Thermo-hydraulic system

TRACE – TRAC/RELAP Advanced Computational Engine

WWER (or VVER) – Water-eater energetic reactor

Table of contents

1. Introduction

The generation of electricity from the nuclear source is present in the energy matrix of thirty countries, being responsible for 10.5% of the electric energy applicable in the world. There are 442 nuclear reactors in operation - totaling 390.5 GWe of installed capacity - and 53 reactors under construction - totaling 56.3 GWe.[1]

The first commercial nuclear generation plants started in the 1960s. Due to the oil crisis in the 1970s, several countries started looking for ways to diversify their energy matrices to reduce their dependence on oil. In this context, a nuclear generation had a great expansion throughout the 1970s and 1980s, reaching 312 GWe of installed capacity in 1989, equivalent to approximately 17% of the electric energy generated at the time.[2][3]

The expansion slowed considerably over the 1990s, mainly in response to accidents at the nuclear plants of Three Mile Island (United States, 1979) and Chernobyl (Ukraine, 1986) and the constant reduction in oil prices. The same happened throughout the 2000s, with fewer new reactor constructions. The stagnation of the growth of nuclear generation can be seen in the Figure 1, which points out the significant reduction in reactors connected to the grid since 1990. [3]

Figure 1. Start of reactors in operation between 1954 and 2018 (WNA, 2018a)

Figure 1 also points to a greater number of reactors being shut down after 1990. The number of shutdowns after 2010 was also significant, especially in non-OECD (Organization for Economic Cooperation and Development) countries. It is worth mentioning that, however, the reactors shut down in Japan after the accident in Fukushima were not considered in Figure 1.
From the expansion of the nuclear sector since the year 2000 took place mainly in countries that do not belong to the Organization for Economic Cooperation and Development, especially in China, where the strong growth in energy demand and the need to reduce carbon dioxide emissions led to a rapid expansion of the nuclear generating complex.[2]

Of the 95 reactors connected to the grid after 2000, the vast majority were in China (44), followed by Russia (12) and India (11). United States, which currently has the largest nuclear park - with 96 reactors - presented only one connection to the grid after 2000.[2]
The deceleration of the nuclear sector in the last two decades is directly related to the decrease in the sector's economic competitiveness. Cases of delays and over-costs during the construction of nuclear plants have become common. The high capital investment, combined with the risks of over-costs, long construction periods and a long time to recover the investment contributed to the reduction of the sector's attractiveness. In parallel, there has been a significant reduction in the costs of other energy sources, such as wind and solar, which has attracted most of the investments in the electricity sector today.[1][3]

In addition, the Fukushima nuclear accident in 2011 in Japan brought even more challenges to the sector. After the accidents, civil society concerns about the safety of nuclear generation increased, leading the governments of countries that have nuclear power plants to reevaluate the safety protocols of the plants in operation. Italy, Switzerland and Germany, the country responsible for the construction and operation of dozens of reactors, decided to decommission all their nuclear plants by 2022, in response to the accident. [1]

Of all the aspects related to nuclear power plants, nuclear safety is what stands out the most. Concerns about possible severe accidents, such as those in Chernobyl and Fukushima, emphasize safety precautions as priority in terms of economic and design. The safety of a nuclear plant depends as much on technical issues as related to the management of the project.

So how to prevent nuclear accidents to even happen in order to preserve everything that surround a nuclear power plant has become more and more important to many countries and challenging to engineering's around the world in due that many tests to check all the aspects of operating equipment and see how well functions they are.

The propose of this work is related to one of the many test that can be made at a function power plant or even during the design project that consists in building a model using TRACE code that can identify eventual leaking due a pipe break between the primary and secondary circuit insight the Steam Generator.

To understand how a pipe rupture causing a leakage and its damages associate to these problems the following chapters will explain breve how a power plant works, its design, why its need attention on the problem studied in this paper by understanding the necessity of a Steam Generator, the flow that passes by the pipes insight and how safety in related in this specific part of the whole process of generating energy from nuclear fissions.

2. Background

This chapter will be introduced the whole functionality of a nuclear power plant in pro to understand the case that is has been investigated and where it happens so the meaning and excuse for the work can be understand.

2.1 Pressurized Water Reactor (PWR)

The Pressurized Water Reactor is present in 299 of the 442 plants operating in the world.[1] Although much more complex, its operating principle is analogous to that of a conventional thermoelectric plant, with the difference that the heat used to generate steam is obtained from the fission of uranium atoms, and not from burning fossil fuels.

There are several models of PWRs, from small reactors, used in the propulsion of nuclear submarines and aircrafts, to large reactors, used mainly for electricity generation.

Its main feature is the use of light pressurized water to remove heat from the reactor core. The power generation process is divided into three circuits: primary, secondary and cooling (or tertiary) water circuit.

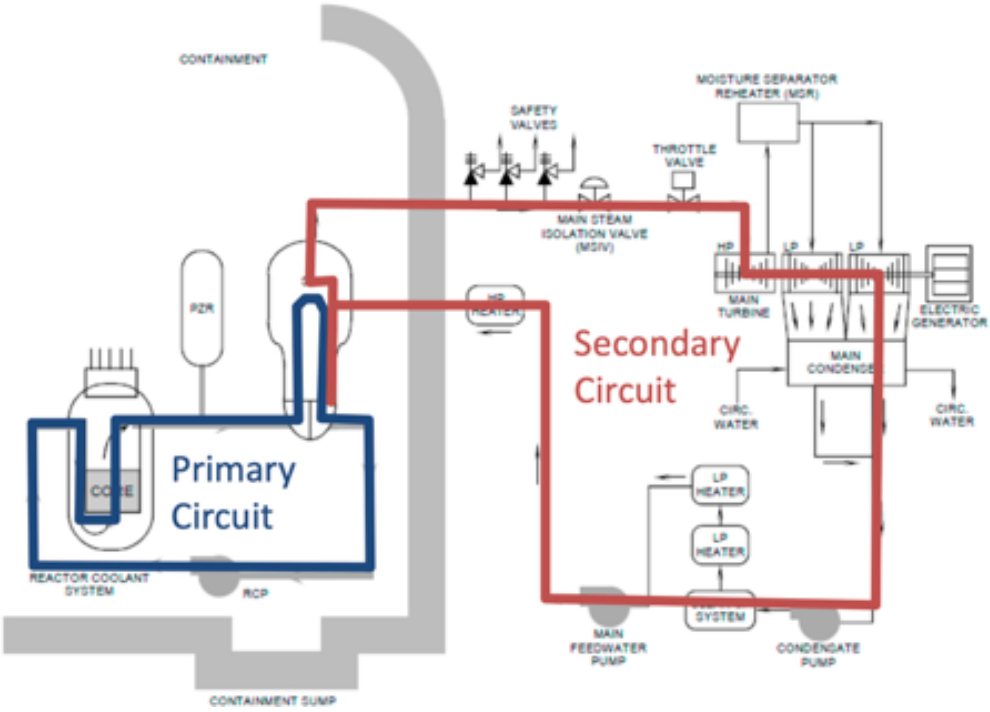

Figure 2. Primary and Secondary circuit of a PWR. [4]

From the figure 2 it's possible to see that the primary circuit is composed of several systems and subsystems, being responsible for generating the heat that will be used to generate electricity.[4] The heat generated by the fission of the uranium atoms is removed by the pressurized water at 155 bar that circulates through the reactor core. After removing heat, the water passes through the tubes of the four steam generators, transferring part of its energy to the secondary circuit.[5]

In general, PWR reactors are formed by 2, 3 or 4 loops, depending mainly on the need for heat exchange between the primary and secondary circuit. For the case of the European Power Reactor, the primary circuit is formed by 4 loops.[5]

The working fluid of the primary circuit - demineralized light water - does not mix with the water in the secondary system, therefore, radiation is limited to that system. The entire primary circuit is contained within the reactor building, which is separated from the external environment by two containment wraps, preventing contact of radioactive material with the

outside. The main components of the primary circuit are: four steam generators, four reactor cooling pumps, a pressurizer and the nuclear reactor.[4]

The reactor core, and the other support and instrumentation components of the core, are housed within the reactor pressure vessel. The pressure vessel of the reactor is cylindrical in shape and consists of two separable parts, the upper one being removed for periodic refills of fuel. There is an inlet for cold water (cold leg) and a hot water outlet (hot leg) for each loop of the reactor cooling system. The cooling water enters the reactor at approximately $296^{o}C$ and receives heat from the core until it reaches $328^{o}C$.[4]

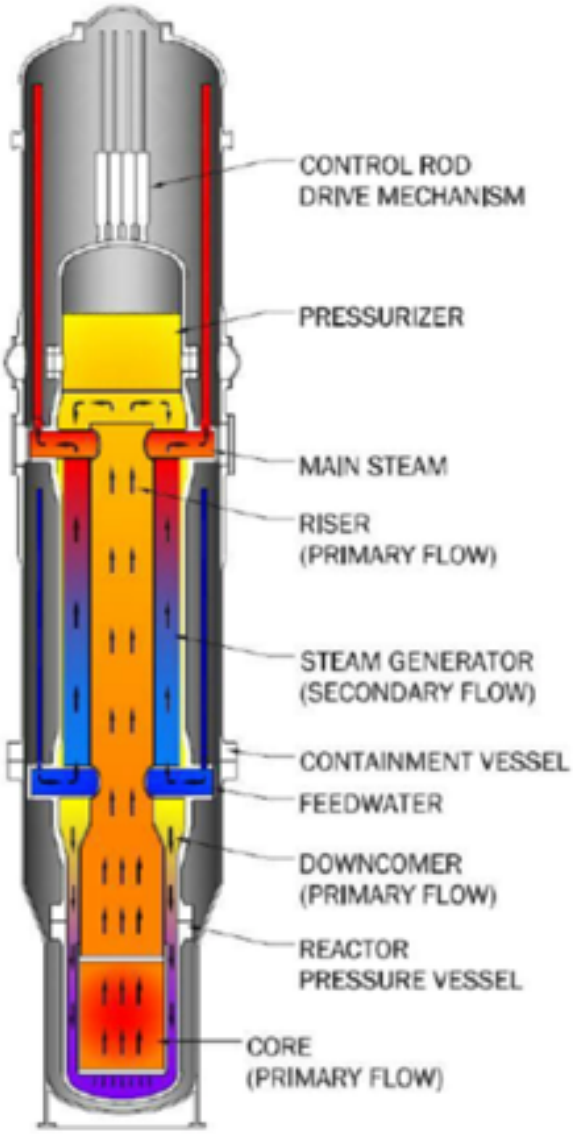

Figure 3. Reactor Pressure Vessel (ANL, 2014)

On top of the reactor core there are 89 sets of control bars, which are inserted into the core when it is desired to control the power of the reactor or in the event of an accident. Each set consists of 24 bars made of neutron-absorbing material (silver, indium, cadmium and boron). In the event of an accident, the bars fall by gravity inside the nucleus, interrupting the fissions.[6]

Primary circuit has four reactor cooling pumps whose function is to circulate the refrigerant from the steam generators outlet to the reactor pressure vessel. They are vertical single-stage centrifugal pumps and are responsible for increasing the refrigerant pressure before entering the reactor.[6]

Reactor Cooling Pump has a fundamental role in cooling the core in the event of an accident. In the case of loss of external power supply, there are safety systems that guarantee additional energy supply to keep the reactor cooling pumps running.

Reactor cooling system also has four steam generators, formed by more than 5000 “U” tubes each. The refrigerant of the primary circuit passes through the tubes, exchanging heat with the feed water that circulates on the side of the hull of the steam generators. Each steam generator has moisture separators, responsible for removing water from the steam before being sent to the turbines. The steam leaves the steam generator at a pressure of 78 bar.[6]

The pressurizer is a vertical pressure vessel connected to a hot leg of the primary circuit, being responsible for maintaining the pressure at approximately 155 bar, when the reactor is operating at maximum power. In its lower part there are the electric heating bars, which when varying the temperature, control the pressure of the primary circuit. At the top of the pressurizer are the relief and safety valves, as well as the spray lines. Therefore, the pressure is kept constant through the electric heating of the bars at the bottom and spraying of water at the top.[6] Figure 4 represents the primary circuit of a four loop PWR.

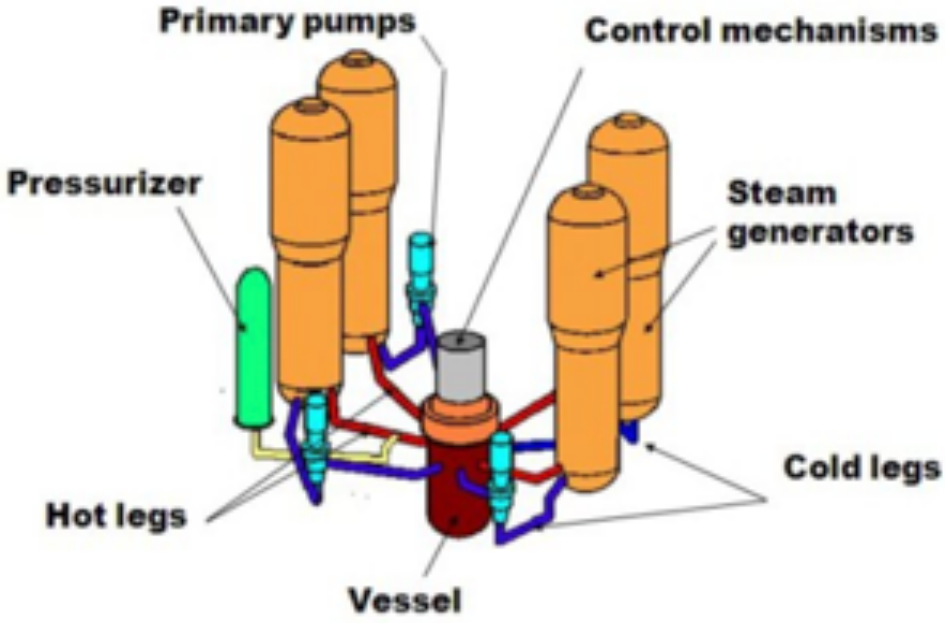

Figure 4. Primary circuit of a four loop PWR. [7]

The secondary circuit is responsible for converting the thermal energy contained in the steam, coming from the steam generators, into electrical energy through the turbines and the electric generator. As the primary and secondary circuit are physically separated by the tubes of the steam generators, the secondary circuit does not contain any radioactive material.[7]

The secondary circuit operates according to a regenerative Rankine cycle and with reheating. Figure 5 represents the Temperature x Entropy diagram of a conventional PWR, while Figure 6 shows the simplified scheme of the secondary circuit of this type of plant.

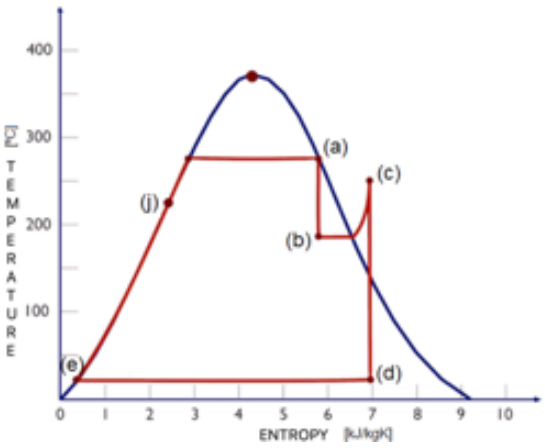

Figure 5. Temperature x Entropy diagram of a PWR.[8]

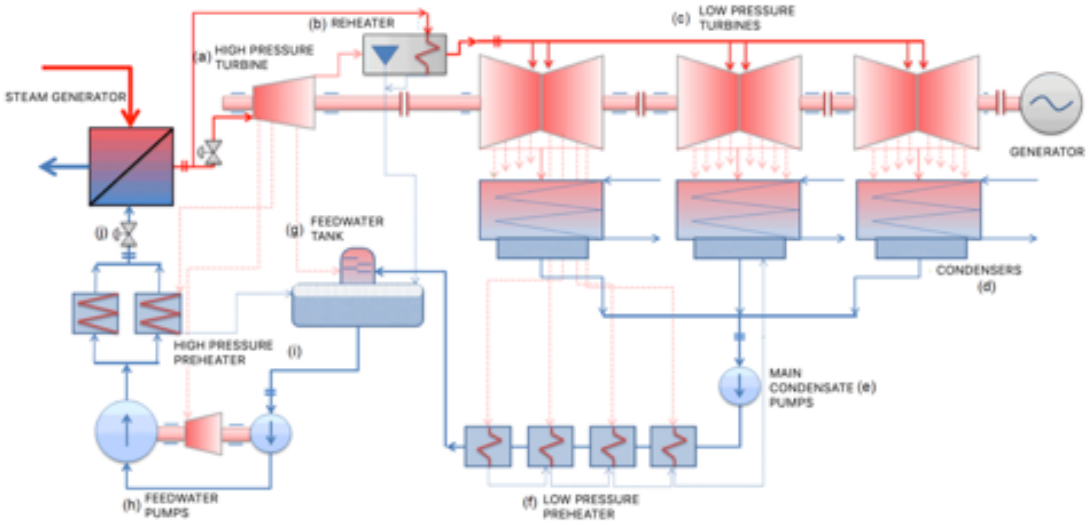

Figure 6. Simplified scheme of the secondary circuit. [8]

The main systems within the secondary circuit are the main steam system and the condensate/feedwater system.

The main steam system starts at the outlet of the steam generator. The high pressure steam leaves the reactor building and is directed to the turbine building, where it enters the high pressure turbine (a), undergoing isentropic expansion. Part of the steam that passes through the turbine is extracted to be used, to reheat the feedwater and part is directed to the reheater (b), which uses part of the steam from the steam generators to overheat the main steam. The superheated steam is then directed to the low pressure turbines (c).[9]

The European Power Reactors have a high pressure turbine, responsible for approximately 40% of the gross electrical power in this type of reactor, and three low pressure turbines, responsible for 60% of the generation. They are coupled to a single 68-meter shaft, where the electric generator is also coupled. [9]

After leaving the low pressure turbines, the steam is directed to the condensers (d), which are operated under vacuum to allow greater use of the energy in the turbines. At the condensers, steam is cooled to a liquid state when exchanging heat with the cooling water of the tertiary circuit, initiating the condensate / feedwater system.[9]

The main condensate pumps (e) direct the water to the low pressure preheater (f), which uses part of the steam extracted from the low pressure turbines to heat the condensate. The condensate flow is then directed to the feedwater tank (g), which behaves simultaneously as a damper for the water-steam cycle and a preheater mixer. At the exit of the feedwater tank, the main feedwater system starts. The condensate flow is pumped by the feedwater pumps (h) to the high pressure preheater (i), which uses steam from the high pressure turbine to heat it. Finally, the main condensate flow is conducted to the steam generators, restarting the cycle (j).[9]

Table 1. General data of EPR reactor (IAEA 2011a, 2020)

General Data	
Name	EPR
Designers	Framatome
Type of reactor	PWR
Purpose of reactor	Commercial
Country of origin	France/Germany
Thermal power	4524 MW (t)
Gross eletrical power	1720 MW (e)
Net eletric power	1630 MW (e)
Plant life time	60 Years
Status	In operation
Primary system fluid	Water
Secondary system fluid	Water
Moderator	Water
Capacity factor	92%
Efficiency	36%
Fuel	UO2
Enrichment	3-5%
Fuel cycle	12 to 24 months
Loops	4
Plant configuration	1 reactor
Plant area	Around 188.00 m2
Data of primary circuit	
Inlet Temperature	296 ºC
Outlet temperature	328 ºC
Pressure	155 bar
Coolant pumps	4
Steam generators	4
Model of Steam Generators	U Tube
Number of tubes	5.980
Heat exchanger area	7960 m2
Fuel pellet	241
Control rods	89
Control of reactivity	Control rods/ Boron
Data of secondary circuit	
Steam temperature	293 ºC
Steam pressure	78 bar

Table 1 shows the general data of an EPR reactor with it's values.

2.2. Water-water energetic reactor (VVER)

In the former USSR, a model of pressurized water-cooled nuclear power reactor was developed, called VVER, a Russian acronym for Water-Water Energetic Reactor, due to the existence of two cooling circuits where the refrigerant fluid is water. There are many similarities between the designs of a PWR reactor already approached previously and a VVER reactor, with a few differences.

The two most obvious differences are in the position of the steam generators (vertical in the PWR reactor and horizontal in the VVER reactor), can be seen by on the figure 7 below:

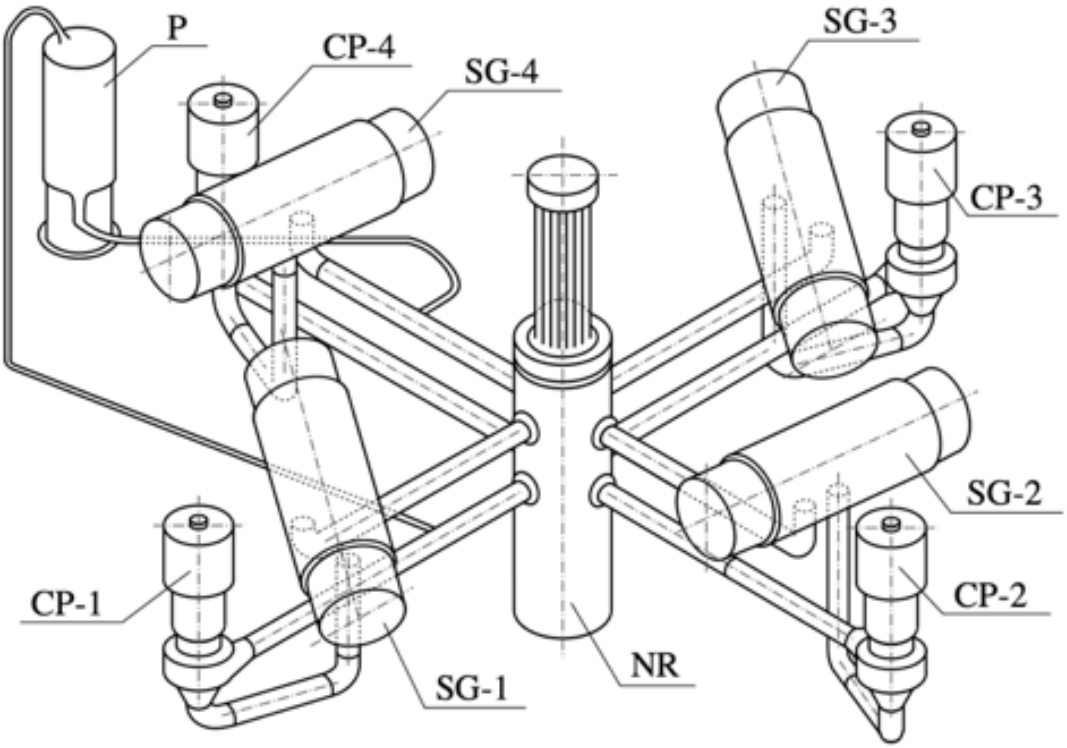

Figure 7. Layout of the four primary cooling circuits and the pressurizer of a VVER-1000. (GLAVA 1)

Where :

SG = STEAM GENERATOR

NR = NUCLEAR REACTOR

P = PRESSURIZOR

CP = PRIMARY PUMP

Another difference is in the configuration of the fuel elements (square cross section in the PWR reactor and hexagonal cross section in the VVER reactor). Typically, the fuel element of a VVER reactor contains 312 fuel rods arranged in a hexagonal arrangement with 11.75 cm of apothem and 3.75 m of active length, fixed by means of spacer grids.[11]

It won't be going further on this matter in fact that it goes beyond the studied on this paper, but it is necessary to mention to explain the differences between the design of the reactor as the study uses references of VVER type of power plant and horizontal types of SG.

2.3 Types steam generator

Nuclear power generation facilities use the most varied models of steam generators. Thus, horizontal or vertical steam generators are used, with straight or "U" tubes, with or without preheaters (economizers), with or without steam separators that can be placed inside or outside the steam generator itself.

2.3.1 Type "U" tubes, horizontal, with internal steam separators

As shown in figure 8, it is observed that the primary fluid travels through the "U" pipe. The feed water (second river) enters the steam generator at the base of the steam generator and flows transversely to the bundle of "U" tubes. It then passes through internal steam separators to ensure dry saturated steam at the turbine inlet. The capacity of this model is limited by the maximum dimensions possible in the manufacture of the containment vessel.[12]

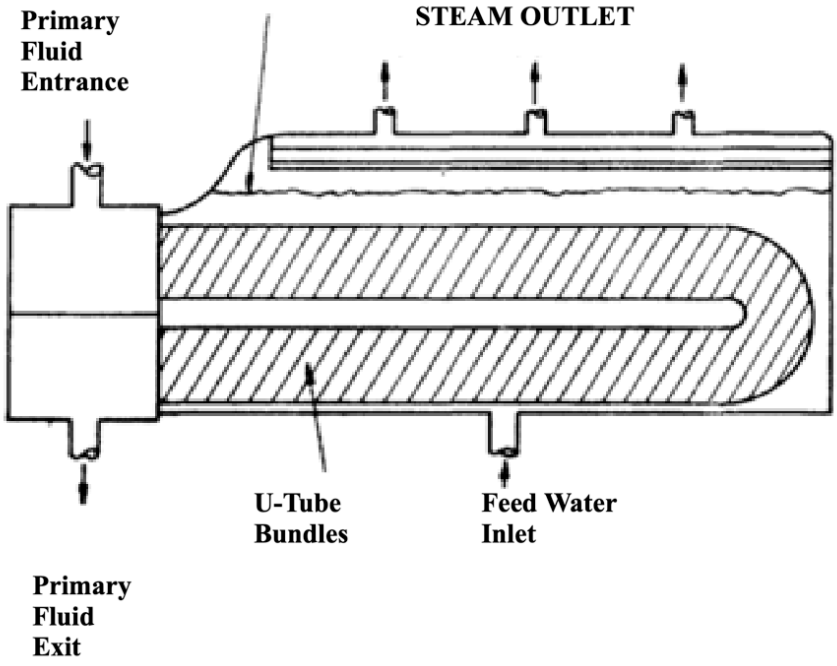

Figure 8. Diagram Of a Pipe and M "U" Type Steam Generator, Horizontal, With Internal Steam Separators.[12]

2.3.2 Straight tube type, horizontal, with external steam separators

The advantage of this model over the one mentioned above is its greater capacity, which is obtained through the use of several containment vessels, as can be seen in figure 9. The primary tubing is contained in the lower vessel while the steam separators are in the upper vessel.

Vertical steam generators were developed with the initial purpose of obtaining a compact and efficient equipment to be used in naval propulsion. The vast majority of nuclear units installed after 1968 use this model of steam generator.[12]

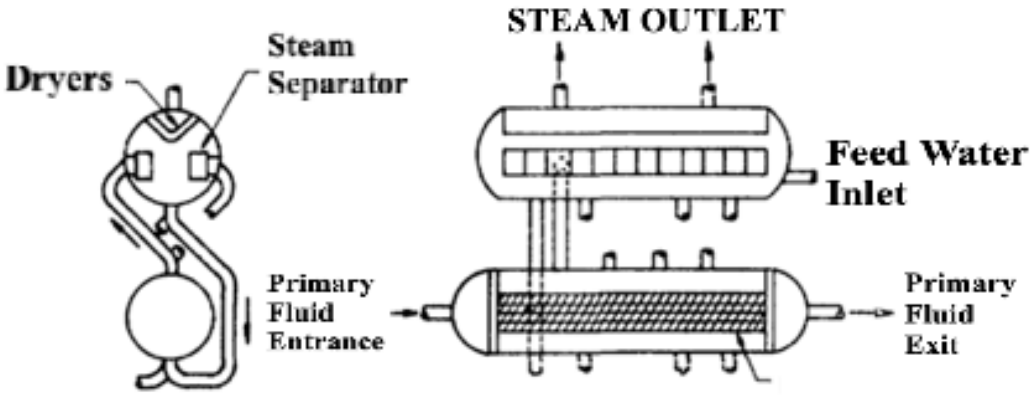

Figure 9. Diagram Of a Straight Pipe Steam Generator, Horizontal, With External Steam Separators.[12]

2.3.3 Type straight, vertical tubes

The development of this steam generator model, shown in figure 10, started when it was desired to obtain superheated steam to feed the turbine. Reactor coolant enters the reactor through its top, then flows down through the tube bundle, leaving the steam generator by its base. The feed water enters the steam generator in its annular section in the form of a "spray", in order to obtain a uniform flow distribution. Then the secondary fluid flows down still in the annular section, penetrating the inner section near the base of the steam generator. In this, the water receives heat until it reaches the state of dry saturated steam, that is, a quality of 100%. Baffles are placed in the superheat region (upper part of the inner section) to obtain high flow velocities transversal to the tube bundle in such a way as to have an efficient heat exchange. The superheated steam leaves the steam generator through a nozzle positioned in the upper annular section. Naturally, when working with superheated steam it is not necessary to use steam separators. One of the disadvantages of this model is its large vertical dimension.[13]

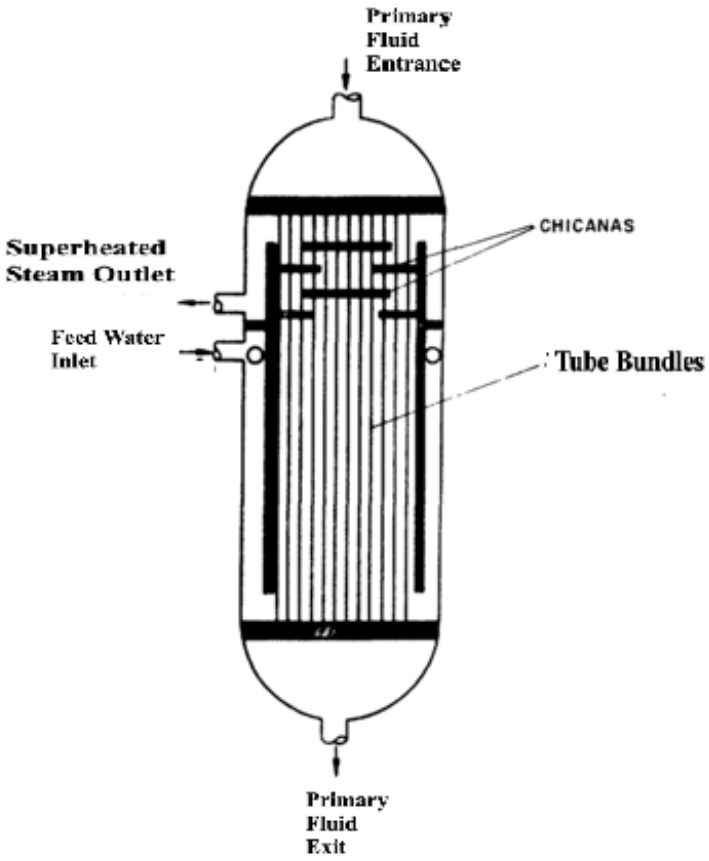

Figure 10. Scheme Of a Straight Pipe Steam Generator Vertical.[13]

2.3.4 Inverted "U" type, vertical, with natural internal recirculation

As can be seen in figure 11, the primary fluid runs through the "U" pipe, entering and leaving the steam generator through its base. The working fluid (feed water) enters the steam generator through a nozzle positioned slightly above the top of the "U" tube bundle, then mixes with the recirculating water. This mixture flows downwards penetrating the effective heating region in a similar way to the vertical straight tube type steam generator. At the end of this, there is a biphasic mixture (liquid-steam) which then passes through the steam separators. Posteriorly the steam leaves the steam generator through the nozzle positioned on top of it and the liquid returns to the annular section.[14]

Some steam generators of this type have a feedwater preheat section which is located at the base of the cold leg of the "U" pipe. This section has horizontal deflectors that are fixed to the tube bundle to cause cross-tube flow. When leaving the preheater, the feedwater penetrates through the hot leg where it mixes with the recirculating water that flows through the annular section.[14]

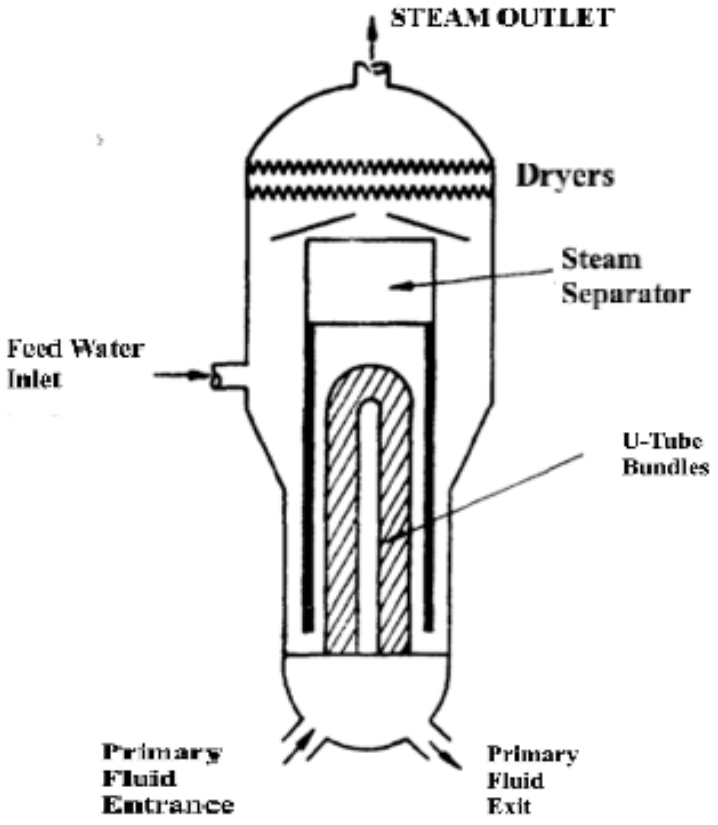

Figure 11. Diagram of an Inverted "U" Type Steam Generator With Inner Natural Recirculation. [14]

2.4 Nuclear safety

The safety systems of a nuclear power plant can be designed by different types, as detailed below (15):

Design barriers – This set of barriers covers all the precautions that are taken even before choosing the location where the plant will be built. It takes into account all the possible risks inherent to the project considering such as earthquakes, tsunamis or even a plane crashing on nuclear installations.

Physical barriers – This category includes all protections used to contain or minimize the radiation levels inherent to the nuclear reactor operation. These barriers, in the case of PWRs, range from the fuel pellet's own molecular structure to the thick steel and concrete walls that surround the entire primary circuit of the plant.

Process barriers – These barriers ensure the safety of human work and its interaction with the machine, establishing work routines and administrative and operational procedures. This category includes items such as periodic testing programs, work procedures (operation, maintenance, engineering, training, chemistry, radiological protection, management) and internal and external evaluation processes.

Organizational barriers – Here are all the legal and institutional controls relating to safety. They include specific national and international laws, the existence of a regulatory body, in the Finish case, the Nuclear Safety Authority (STUK), and agreements with national and international bodies.

These barriers aim to ensure both the radiological safety and the physical safety of nuclear power plants. The definition of these two concepts is given below (INSAG, 2010):

- Radiological safety (nuclear safety): obtaining adequate operating conditions, preventing or mitigating the consequences of accidents; resulting in the protection of workers, the public and the environment from the negative impacts of radiation.

- Physical security (nuclear security): prevention, sabotage, unauthorized access, illegal transfer or other malicious acts with nuclear material and radioactive substances.

Safety is strongly connected acceptance of nuclear energy by the society. The severe accidents that happened in the past have raised questions about the possibility of future accidents with the use of nuclear power plants to generate energy. It is interesting to note that the generation of energy from fossil fuels, which face less resistance from society in terms of safety, have a higher number of fatal accidents, both for workers and the general public.[17]

In this context, increasingly advanced technologies are collaborating to further increase the safety of nuclear reactors. On the other hand, this leads to more expensive enterprises, which today employ several complex systems dedicated exclusively to preventing or mitigating accidents.

Nuclear safety is also strongly associated with economic and political factors in countries that have plants. Still taking the Fukushima accident as an example, the total amount spent by the Japanese government on mitigating the consequences of the accident, until 2015, exceeded 13 billion dollars. In addition, Germany, one of the countries with the greatest expression in the nuclear sector, decided to decommission all its reactors by 2022 as a result of the accident, deeply affecting the country's energy planning. Italy and Switzerland also decided to end their nuclear programs. It is worth mention that there is no record of accidents with radiation release in those country's plants. It is evident, therefore, the economic and political impacts resulting from severe nuclear accidents even in those countries that were not directly affected by the accident.[18]

Public opinion is extremely important for the nuclear sector, being one of the main factors responsible for the slowdown in investments after the Chernobyl and Fukushima accidents. The acceptability of nuclear energy was the subject of studies by Chao-jun et al. (2013) and Roh and Lee (2017), who indicated its direct relationship with safety. It was noted that public acceptance of nuclear energy has a direct impact on the development of the sector, as well as the establishment of new safety goals.[18]

2.5 Trace code

In a lack of a facility where the experiment could be performed, the support of a program were needed where the simulation could be performed, and the results obtained simulation the real life experience.

TRACE (TRAC/RELAP Advanced Computational Engine) is a thermo-hydraulic code designed to consolidate and extend the capabilities of the 3 legacy NRC security codes: TRAC-P, TRAC-B and RELAP. It is capable to analyze small and large LOCAs (Loss of Coolant Accidents) and transients for both pressurized water reactors and boiling water reactors (PWR and BWR). It is also capable of modeling thermo-hydraulic phenomena in

one or three dimensions, being currently the main thermo-hydraulic analysis tool of the NRC. TRAC-P and TRAC-B are analysis tools of transients and LOCA for PWR and BWR, respectively, and were incorporated into the TRACE, being therefore in disuse separately. RELAP (Reactor Excursion and Leak Analysis Program) is a tool for analyzing small LOCAs and transients in PWR and BWR, modeling thermo-hydraulic phenomena in one-dimensional volumes.[19]

2.5.1 Trace code overview

This program also makes it possible to detect the presence of choked flow within the volume with a smooth change in the passage section. Essentially, it calculates the values of single- or two-phase flow parameters in a one-dimensional model at which a choked flow effect can occur. It then compares the predicted parameters of this flow with the parameters at the moment in question. The accuracy of this calculation can be improved by increasing the nodalization, i.e., increasing the sections into which the one-dimensional element in question is divided. This, however, significantly increases the number of calculation operations, and hence the calculation time. This is why when using TRACE code, it is necessary to clearly define the degree of calculation accuracy prior to model building, so as not to get excessive error, and at the same time overloaded calculation part.[20]

As stated above, the calculation considers the state of the flow in question, and this will determine which calculation base will be applied to a particular state. This is why it is vital that the software can determine exactly which model to use for the calculation[20]:

- Single-phase vapor flow

- Single-phase subcooled liquid flow

- two-phase flow (gaseous and liquid)

Also, since TRACE code identifies the presence of choked flow at the cell edge, it can be determined for each specific cell where this is required.

2.5.2 Single-phase subcooled liquid flow [20]

As mentioned earlier, the TRACE code first calculates the potential velocity and pressure parameters at which choked flow can occur and then makes a comparison with the momentum values at the cell wall under investigation.

A modified Bernoulli model is used as a model for determining the choked flow for a subcooled fluid. Based on the assumptions of no friction of liquid against the wall and incompressibility of liquid, the liquid velocity equation takes the following form:

$$V_t = \left[V_{up}^2 + \frac{2(p_{up}-p_t)}{\rho_l}\right]^{\frac{1}{2}} \quad (1)$$

where p_{up} and p_t are upstream and throat pressures respectively, V_t is liquid velocity in throat, V_{up} is upstream liquid velocity and ρ_l is liquid density.

Based on the theoretical basis of liquid flow behavior, at homogeneous and equilibrium sound velocity in the medium, as well as at the maximum of Bernoulli's expression, the criterion for the origin of the critical medium flow has been established.

$$V_t = Max\left\{a_{HE}, \left[V_{up}^2 + \frac{2(p_{up}-p_t)}{\rho_l}\right]^{\frac{1}{2}}\right\} \quad (2)$$

Nonequilibrium conditions can cause a nucleation delay, when nucleation pressure is lower than saturation pressure, p_{sat}. In TRACE, the delayed nucleation model is implemented based on the Alamgir and Leinhard model modernized by Jones and Abuaf, allowing the pressure at the cell boundary to be determined from the saturation pressure value.

$$p_t = p_{nuc} = p_{sat} - Max\left[0.0, 0.258\frac{\sigma^{1.5}\left(\frac{T_l}{T_c}\right)^{13.76}\sqrt{1+13.25\left(-\frac{1}{1.01325\cdot 10^{11}}Dp\right)^{0.8}Dt}}{(kT_c)^{0.5}\left(1-\frac{\rho_g}{\rho_l}\right)} - \right.$$

$$\left. -27(0.072)^2\left(\frac{A_t}{A_{up}}\right)^2\frac{\rho_l V_t^2}{2}\right] \quad (3)$$

where k is Boltzmann constant, ρ_g and ρ_l are gas and liquid densities at the edge cell respectively, V_t is cell-edge velocity, A_t and A_{up} are areas of throat and upstream cross sections areas respectively and σ is surface tension.

The iterative solution of the system of equations 2 and 3 leads to the determination of the chocked flow occurrence velocity value. By comparing this assumed value with the actual velocity at a given point in time, a decision is made as to whether chocked flow has occurred or not.

2.5.3 Single-phase vapor flow [20]

The system for determining choked flow in this medium is based on the calculation of three parameters: throat pressure, downstream throat temperature and then fluid choking velocity.

The throat pressure value, p_e, and throat temperature, T_e, are directly related to the stagnation pressure, p_0, and temperature, T_0, respectively and are calculated using the formulas below.

$$\mathrm{p_e} = \mathrm{p_0}\left(\frac{2}{\gamma+1}\right)^{\gamma/\gamma-1} \quad (4)$$

$$\mathrm{T_e} = \mathrm{T_0}\left(\frac{2}{\gamma+1}\right) \quad (5)$$

where γ is specific-heat ratio.

Once the above calculations have been made, the software code then considers two possible outcomes:

- Temperature, T_e, above the saturation temperature at the pressure, p_e;

- Temperature, T_e, is equal to or lower than the saturation temperature at the pressure, p_e.

In the first case, it is assumed that the fluid flow in the throat is in a superheated state. Based on this, relying on the continuity equation, which in combination with the relation for an ideal gas gives the expression represented by Equation 6, the software code calculates the velocity at which choked flow can occur.

$$V_{ge} = \sqrt{\frac{2\gamma}{\gamma+1} RT_0} \quad (6)$$

where R is the gas constant

In the second case, the fluid flow is not in a superheated state. To calculate the choked flow velocity, an iterative parameter calculation method with maximization of liquid flow along an isentropic straight line is used. The main assumption of this method is that condensation lag is not considered in calculations and is assumed to be equal to zero for steam transition to two-phase state in throat.

2.5.4 Two-phase flow (gaseous and liquid) [20]

This is a much more time-consuming calculation for a TRACE code program. The presence of two-phase flow indicates a large difference in sound velocity, density, and hence flow velocity.

The methodology is based on the extended model developed by Ransom and Trapp, which considers the presence of noble gases and the system being in a non-equilibrium state, where

the liquid phase can change into gaseous phase and vice versa. However, within the code it is assumed that these transitions are equivalent and compensate for each other.

The computational apparatus in the presence of phase separation is cumbersome and is accurately described in the manual (TRACE V5.0 THEORY MANUAL, Appendix C). Eventually the critical point is determined by solving a fifth order polynomial and determining its roots.

$$determinant\left(\underline{A}\lambda - \underline{B}\right) = 0 \quad (7)$$

The occurrence of choked flow is characterized by the stationary state of the signal propagating with the highest velocity, relative to the fluid. In this case, the value of the real part of the characteristic root is zero. However, the mathematical apparatus is difficult to solve analytically using TRACE code, so the solution is done numerically. The advantage of this method is that it is more generalized and allows calculations to be made based on all necessary assumptions.

2.6. Thermal hydraulics

To also understand the significance of flow phenomena to nuclear reactor design and safety, this is the part where it finally come through where the findings of the whole word will appear. It's known that the water increases its temperature and by changing its properties basically do the important part into a NPP. Getting familiar with this behavior insight the reactor can become closer and closer to what actually happens, and all this changes insight can sometimes although it's not actually possible to see but can be more evident so in case of something happens it's possible to know what can be done.

2.6.1. Critical Flow

Critical flow, or choking flow, is the maximum flow obtained under given upstream stagnation conditions. Critical flow occurs in the throats of relief and safety valves whenever fluid is discharged from a pressurized vessel or piping system. Which makes its analysis and evaluation necessary since its impact has great relevance on the safety of a nuclear reactor.

Critical flow models are considered an important module in all thermo-hydraulic system (THS) codes, with each model having its application scope. In water-cooled nuclear reactors such as CANDU and PWR, where high pressure subcooled water is used to generate steam, as a liquid flows through a channel from high pressure to low pressure, the saturation temperature drops at along the channel. If the saturation temperature drops below the temperature of the liquid, some of the liquid will turn to vapor.

A large change in the sonic velocity of the liquid-vapor mixture will limit the flow through the channel because steam has a much lower sonic velocity than water. In the case of a LOCA, when too much emptying occurs in the primary circuit and the pressurized sub-cooled water approaches the range, it turns to steam, resulting in choke. If choke did not occur, the reactor's water supply would quickly run out. Therefore, the cooling capacity and integrity of the core during a LOCA depends on the throttling. If SG tubes has/have small cracks and even breaks, cause loss of coolant from the primary side to the secondary side.

A small or large breach in a reactor's containment building can leak coolant from the primary side of the reactor. Therefore, blocked flow plays an important role not only in a nuclear power plant's designed safeguards, but also in normal operation. In the event of leakage through the SG pipes to the secondary side of the plant, secondary flow radiation detection measurements are taken and calibrated to predict an increase or decrease in leakage through the SG pipes. Therefore, it is of great interest to be able to quantitatively predict these flow rates with great accuracy, not only the leakage rates of thin-walled (<2 mm) but also thick-walled (2 mm) steam generator tube leakage diameter of 3.175 mm and 1. 3 mm with defect sizes found in SG tubes as well as leakage rates after break.

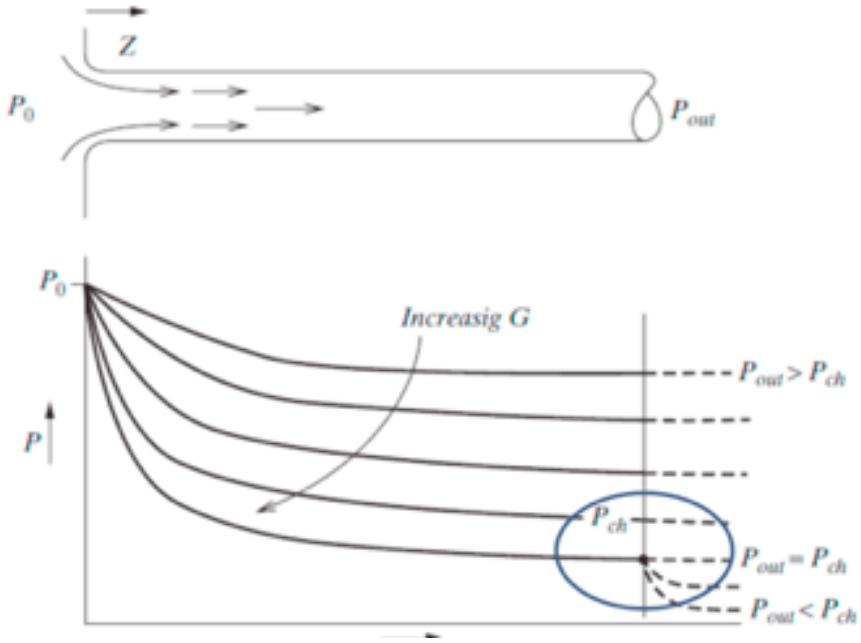

Figure 12. Example of critical flow curve behavior.

Because throttling criteria can only be derived for compressible flow, throttling occurs at the point where the local flow velocity reaches the local speed of sound. Information about downstream conditions cannot travel upstream faster than the speed of sound; in choked condition, the information “stands still”. The explosion is associated with a very large opening in the side of a pipe.

3.6.2. Critical flow for homogenous two-phase flow: basics

The homogeneous flow assumption implies no phase slip. This is a reasonable approximation for high speed flow (close to critical point speeds). The homogeneous flow also assumes thermal equilibrium (=saturation).

− Phase (local) densities depend only on (local) pressure

− Thermal equilibrium is also approximate, because the reduction in nozzle pressure must be compensated by evaporation, but nucleation and bubble growth take time.

If bubble nucleation times were very long, then a low rate of energy release would result. It is clear that if bubble nucleation times were very long, a low rate of energy release would result and reduced energy demand; however, it is.

Rapid depressurization in the stream is always a non-thermal equilibrium event (as it is boiling) Despite known inaccuracies, the homogeneous speed of sound gives a good idea of the order of magnitude of critical two-phase flow rates B.

Critical pressure is defined as the pressure existing at the exit edge of the pipeline when it remains constant despite a decrease at the rear. According to this definition, the critical pressure is greater than the back pressure and for two-phase conditions below the saturation pressure. Critical mass flow and critical depressurization rate calculations are of high significance in the areas of nuclear reactor safety. They are used to estimate the depressurization of the Reactor Cooling System, the pressure build-up in the containment and the level of the core coolant.

Two-phase critical out-of-equilibrium flow stages:

1- The flow of subcooled liquid at constant temperature and uniform pressure drop. In this case, the flow of the incompressible liquid causes a delay in the boiling of this liquid, which, being in thermal imbalance, begins to boil in the pipe of uniform cross section.

2- The boiling it is characterized by a sharp increase in pressure drop and most of the energy for vaporization makes the temperature of the liquid almost constant.

These are the two phases of critical water pressure. Water serves as a coolant in the vast majority of nuclear power reactors around the world.

2.6.3. Void fraction

Void fraction is defined as the ratio of the volume of the gaseous phase occupied in a channel to the total volume of the channel. A nucleated bubble grows due to the pressure difference between the two phases. An expanding bubble is affected by shock fronts from other bubbles.

The propagation of the phase transition front is affected by a force that moves a bubble wall causing mass fluid movements as well as temperature gradients in the plasma. This force is not simply given by the pressure difference, since first, the temperature varies along the wall. Deviations of particle distributions from their equilibrium values within the wall give rise to a frictional force.

The void fraction is of importance in two-phase flow as it influences key physical parameters such as viscosity, pressure drop and heat transfer.

3. Computer Modelling

In this section will be explained what has been done in this experiment and how it will be obtained the results.

A series of computer modelling were performed in pro to be analyzed with the simple task of identify the critical flow and where it happens, the void fraction and its behavior during the phenomena.

In this report were conducted to build a model that simulates critical flow through different sizes of pipes with different initial values simulating a working Steam Generator. Differences pressures in the inlet with the same pressure at the outlet of the pipe by using different lengths of pipes can lead us to different results and the propose of this experiment it's to identify.

3.1 Initial values

To start to model, initial values used was suggested by the supervisor on this case. To start modelling the reference used was of a EPR type of reactor that has in normal operation The table below gives the data used:

Table 2: Initial Values

Tube lengths [m]	Primary pressures [MPa] as changing boundary				Temperature [deg_C] Constant	Secondary pressure [MPa]
0,8	15,50	15	14	13	328	7,8
5	15,50	15	14	13	328	7,8
10	15,50	15	14	13	328	7,8
15	15,50	15	14	13	328	7,8
20	15,50	15	14	13	328	7,8
22,24	15,50	15	14	13	328	7,8
25	15,50	15	14	13	328	7,8

As it can be seen, there were 28 different simulation each one of them with its own data.

For all the cases de pipe internal diameter remained the same:

$$D_{in} = 16{,}84mm \quad [1]$$

3.2. Reference model

The model to help into the calculation has already been mentioned, done by TRACE code and flowing the initial data given.

All the 28 different calculations were performed in the same model design, and its only difference were the size of the pipes that have been changed during the simulations, but the design were quite the same. Here is an exemple of how it looks like.

Figure 13. Trace code modeling used in during the calculations.

3.3 Modeling procedure

The cases of calculations with constant boundary conditions to get the information what are the scales of flows and where the "critical throat" is formed if any.

It starts with flow when primary pressure varies in range normal operation pressure and hot leg saturation pressure (one phase boundary option). Hot leg pressures 15.5 – 12.5 MPa (and cold leg case 15.5 – 8.1 MPa). Suitable number of different pressures between the range. Assume here that temperature and secondary pressure remain constant.

When pressure goes near to saturation bubble formation is probably beginning. To follow if flow is critical or choked if any and where the location is and also the void fraction distribution along the tube.

The simulation of each case lasted 1000 seconds.

Conduction the simulation, it was decided to let the simulation runs as normal for 2 seconds, and right after that the break happens, it means that the break happens, and the pressure drops from the hot leg compared to the cold leg. So, after 2 seconds until 100 seconds were analyzed to see if any special phenomena happened, if the flow become critical.

Nodalization variations also possible and it was used. Some cases as described the phenomena to be really fast, there was not possible to see from the initial nodalization/cells choose. At first it was decided to use 50 cells, basically divide the pipe size into 50 parts and analyze each part separately and see the phoneme but some cases there was no phenomena shown. As the simulation was performed and programmed to see the the phoneme, designed intended so the phenomena happens, it was necessary to increase the number as it has happened in some cases.

It was increased from 50 cells to 100 cells and only one specific case the need of increase even more was needed. So, it was increased once again from 50 to 100 and finally to 150 cells.

All the cases were the number of cells were increased will be described during the results section.

For each length vary with different pressure boundaries.

4. Results

This section will be used to illustrate all the results found by the experiment where is clear that the critical flow appearance, as mentioned before there was several cases where it appears for each of the initial data used in the model.

4.1. Critical flow and void fraction for pressure 15.5 MPa

Here will be presented the results for all the different pipe sizes with the same initial pressure 15.5 MPa.

4.1.1 Results for pipe size 0,8m

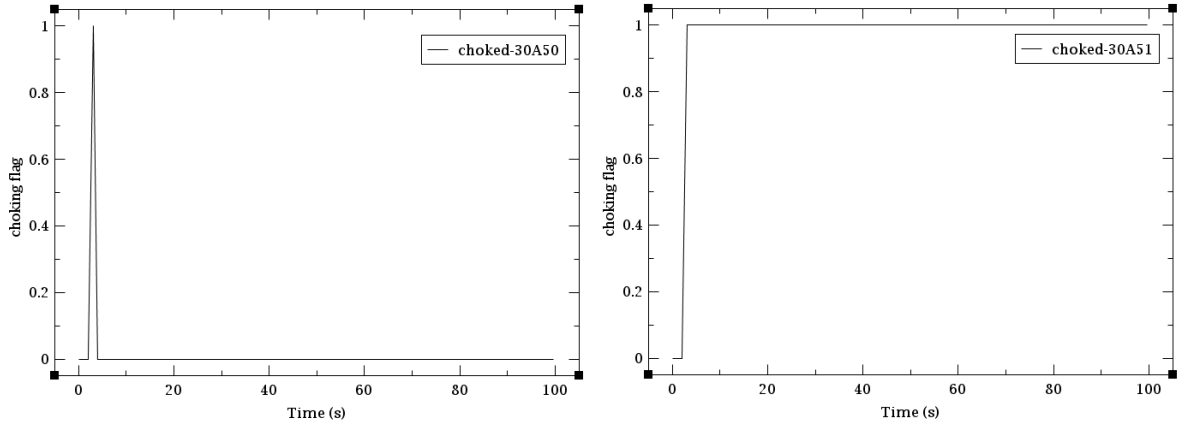

Figure 14. Graph of Critical Flow appearance of Pressure 15,5 MPa, pipe size 0,8 m on cell 50 and 51.

As it can be seen from the calculations showed in the figure 14, we have an appearance of the phenomena immediately when the break happens after 2 seconds. Two different results as in cell number 50 the phenomena happens really fast and soon disappear, as for cell 51 the phenomena continue over the time.

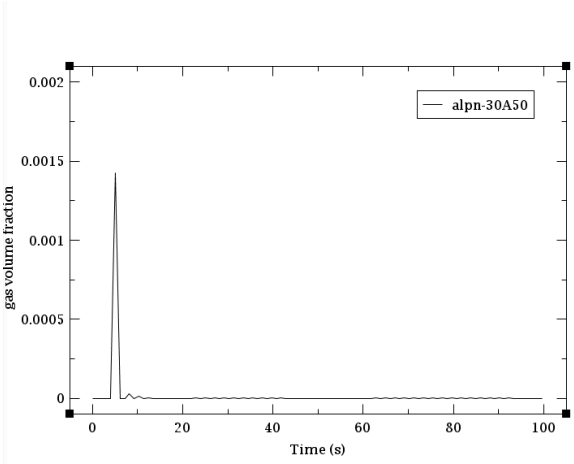

Figure 15. Graph of void fraction on pressure 15,5 MPa, pipe size 0,8m.

As it can been seen from the figure 15 there will be an appearance of a void right when the break happens, but as the scale shows us to be small and really fast not getting even close to 0.1.

4.1.2 Results for pipe size 5m

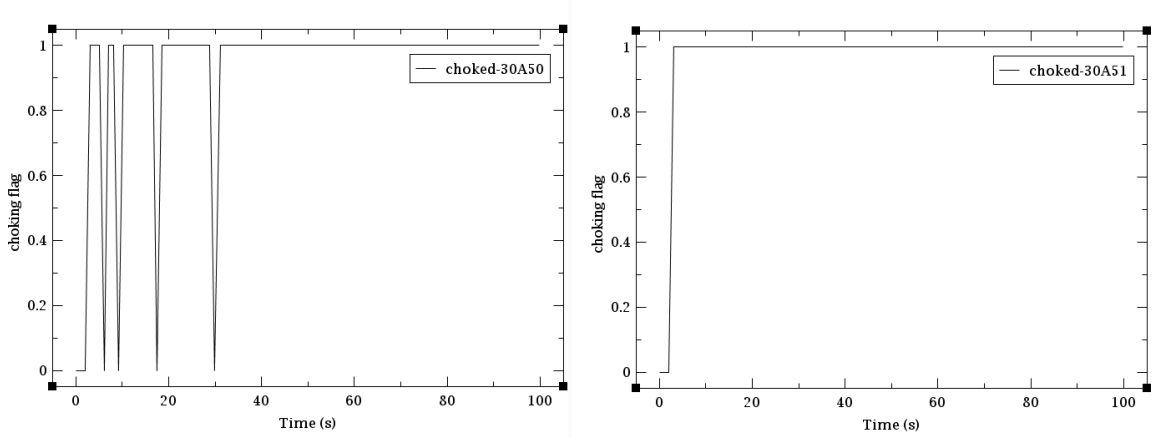

Figure 16. Graph of Critical Flow appearance of Pressure 15,5MPa, pipe size 5m on cell 50 and 51.

As it can be seen from the figure 16, the modelling showed also an appearance of the critical flow phenomena in two cells where in cell number 50 we can see the behavior is a bit different where the phenomena appear right after the break and normalize and goes again increasing its peaks and cell number 51 we have the phenomena happening along the time.

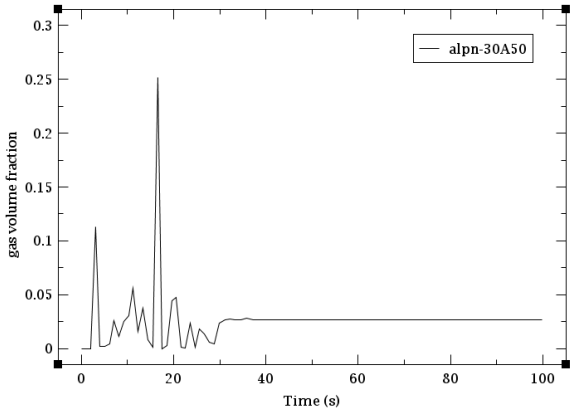

Figure 17. Graph of void fraction on pressure 15,5 MPa, pipe size 5m.

From the figure 17 we can see a bigger formation of void when comparing with the previous modelling, we have a bigger appearance right after the break that soon its normalized.

4.1.3 Results for pipe size 10m

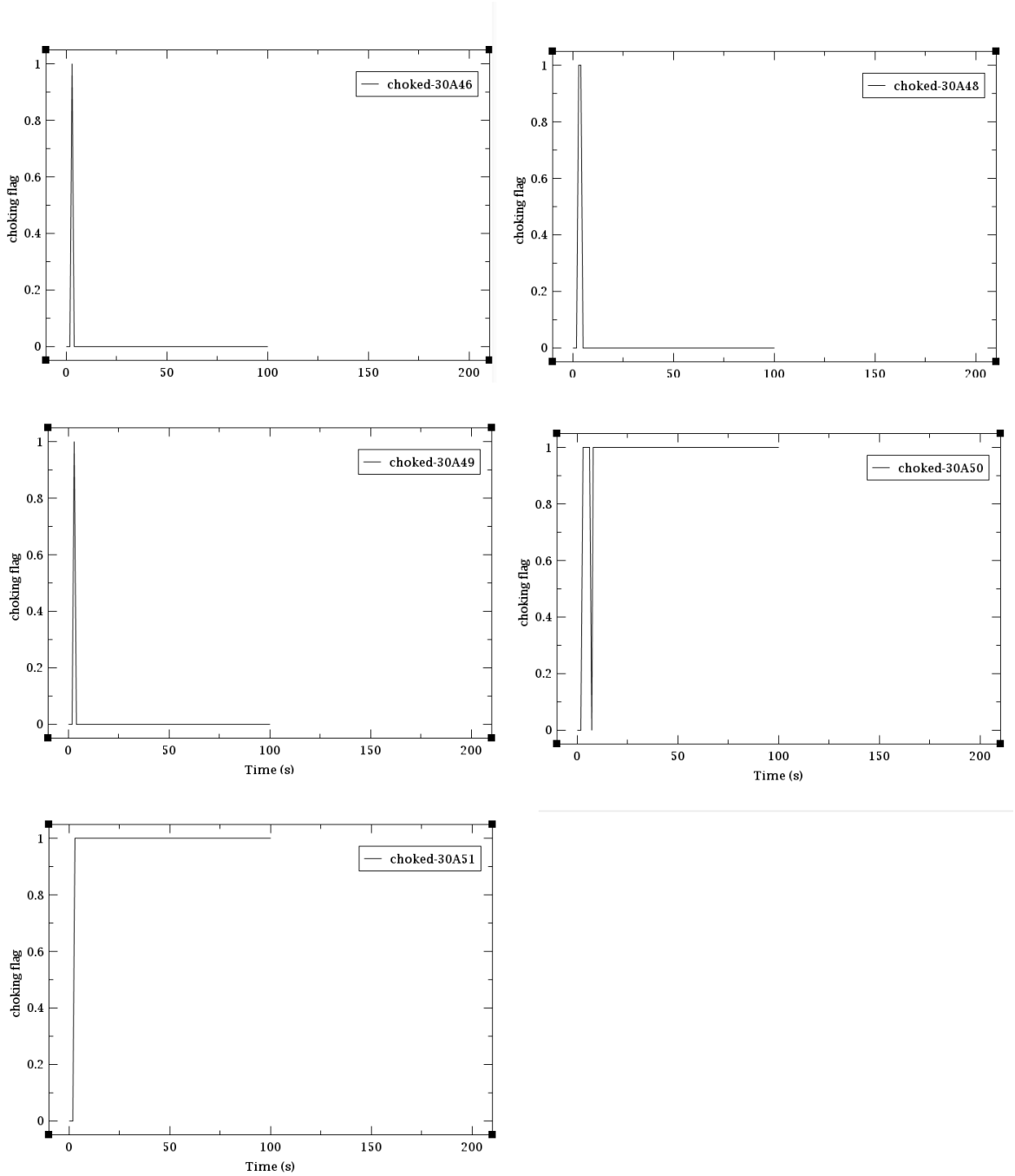

Figure 18. Graph of Critical Flow appearance of Pressure 15,5MPa, pipe size 10m on cell 46, 48, 49, 50 and 51.

Modelling results showed us the phenomena happening in more cell than the previous ones, showing the same result, the phenomena appears right after the break in 2 seconds and soon

disappear with exception of cell number 50 and 51 that the shape of the graphic is a little different.

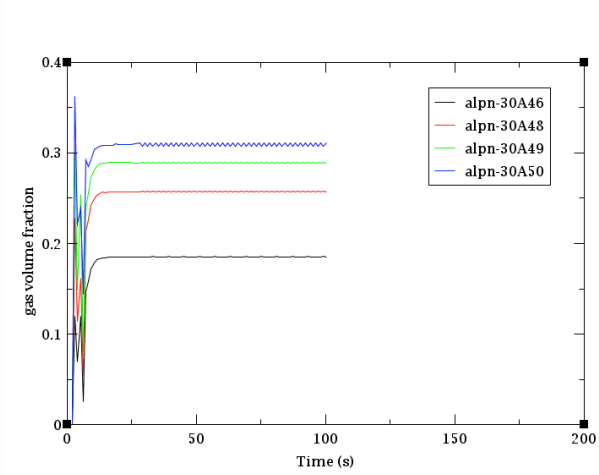

Figure 19. Graph of void fraction on Pressure 15,5 MPa , pipe size 10m.

From the modelling it's possible to notice that the void appearance right after the break has its formation that last during the whole time bigger in the cell 50 and as void is measured in scale 0 to 1, 0.3 is a bigger value so far.

4.1.4 Results for pipe size 15m

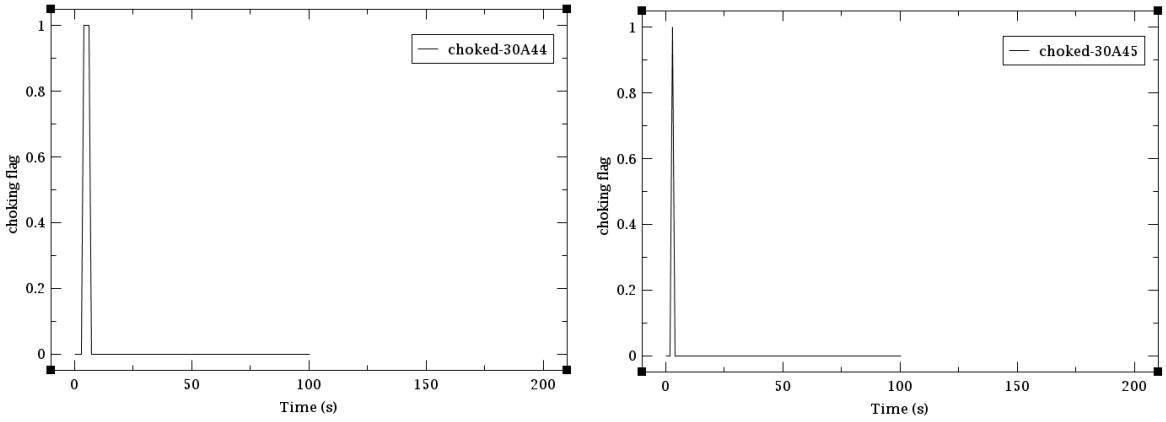

Figure 20. Graph of critical flow appearance of pressure 15,5 MPA , pipe size 15 m on cell 44 and 45.

Different from the previous results that has tended the phenomena to appears more in the last cell, here we have critical flow in the cell 44 and 45 with the cell 44 during a little more than cell 45. In both cases the phenomena is really has and doesn't last longer.

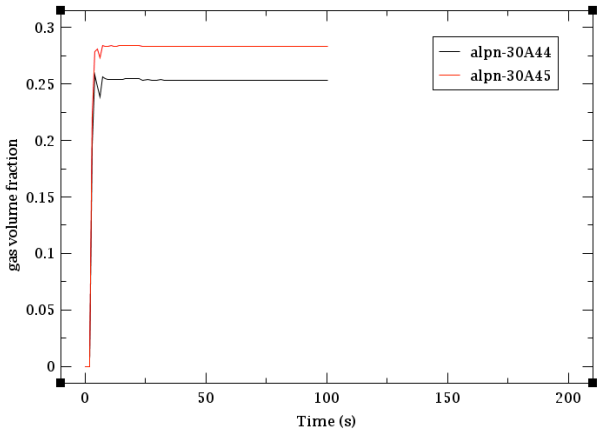

Figure 21. Graph of void fraction on pressure 15,5 MPa, pipe size 15 m.

In both cases is possible to see the formation of void right after the break that continues along the time as it's possible to notice that in the cell 45 the void in a little bigger than in the cell 44.

4.1.5 Results for pipe size 20m

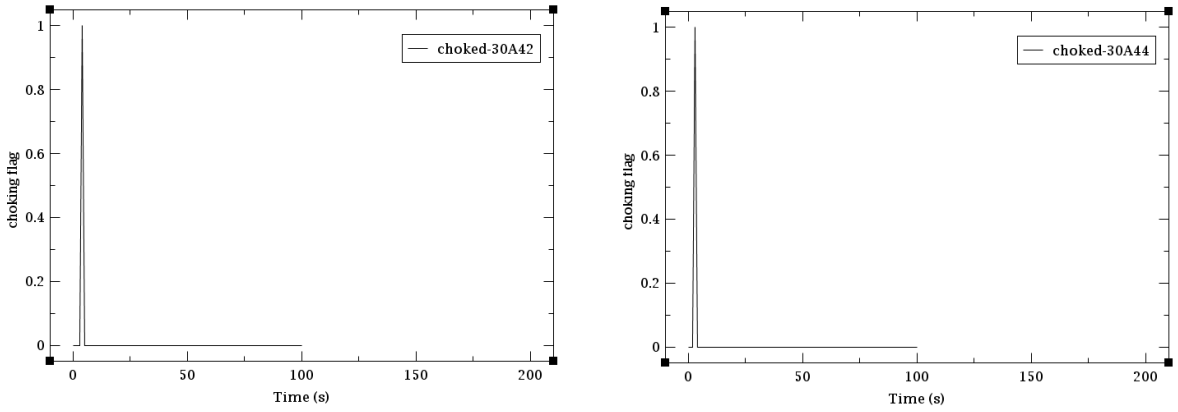

Figure 22. Graph of critical flow appearance of pressure 15,5 MPa, pipe size 20m on cell 42 and 44.

As it can be seen from the results in the figure 22 we have an appearance of the critical flow in two cells that doesn't last longer, just right after the break and then disappear.

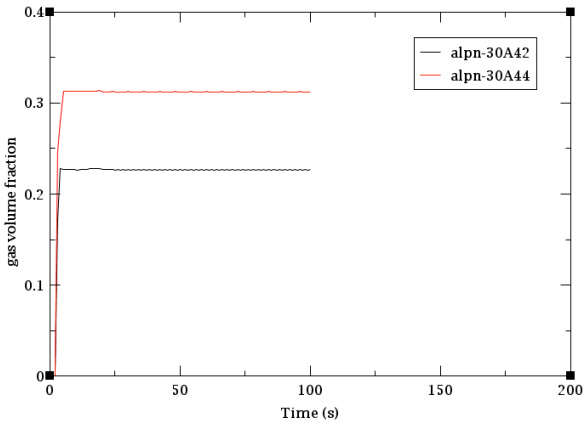

Figure 23 Graph of void fraction on Pressure 15,5 MPa, pipe size 20m.

Although the appearance of the critical flow in the two cells could be seen that doesn't last longer, there is a significant amount of void in those two cells, as the cell 44 its over 0.3 in a scale of 0 to 1 looks significant.

4.1.6 Results for pipe size 22.24m

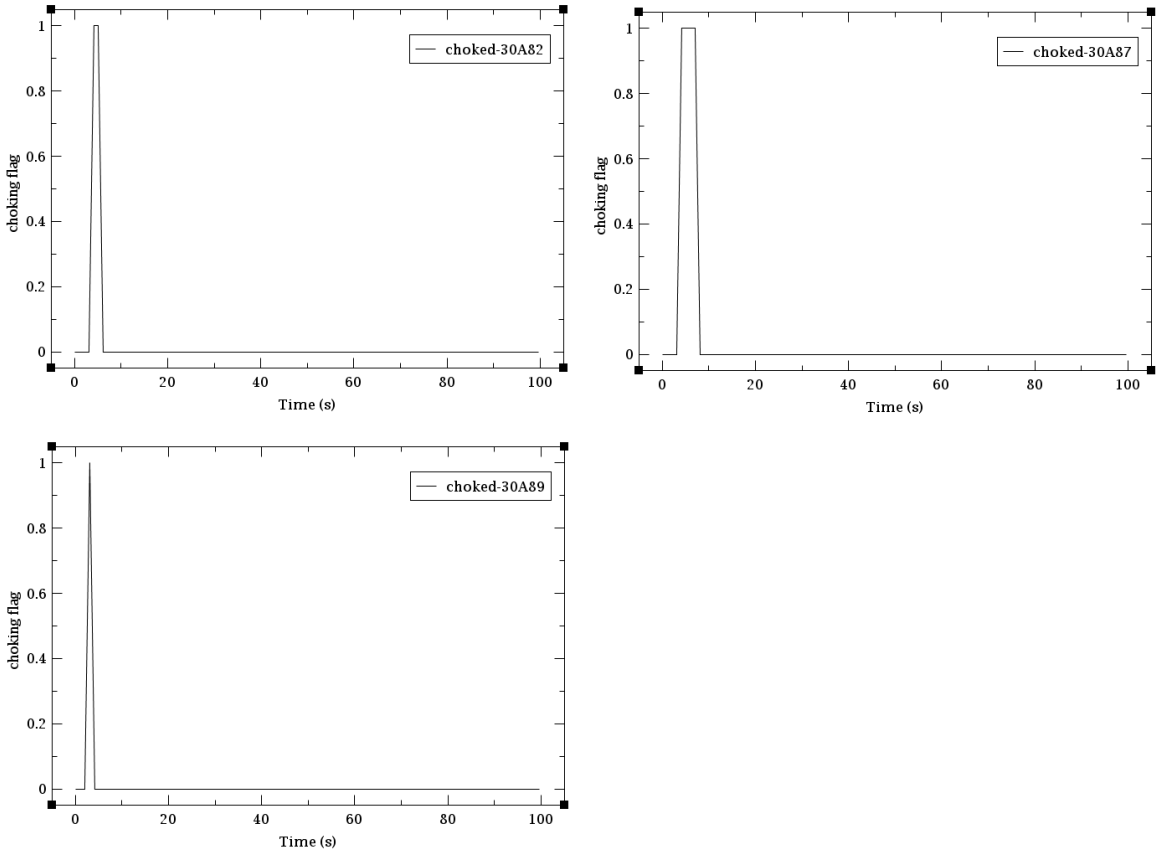

Figure 24. Graph of critical flow appearance of pressure 15.5 MPa, pipe size 22.24m on cell 82, 87 and 89.

Some special cases instead of dividing the pipe into 50 cells to find the critical flow, the need of increase the number of cells were necessary, and this is one of the cases where instead of using 50 cells, 100 cells were used and by that was possible to see. As the results shows in the figure 24, we have the phenomena in tree cells where in all the phenomena appears right after the break with different shapes but none of them continues after 10 seconds.

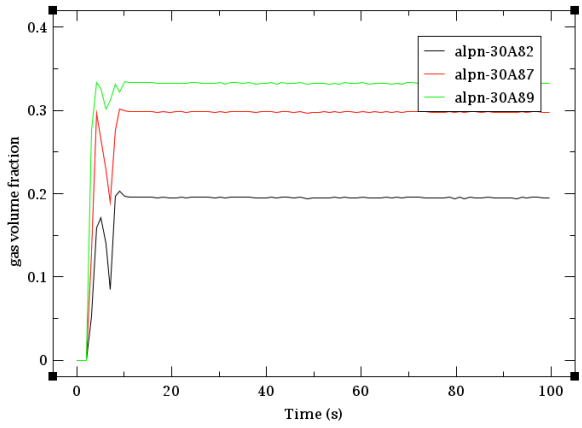

Figure 25. Graph of void fraction on Pressure 15.5 MPa, pipe size 22.24 m.

From the figure 25 we could see that there is a formation of void in the cells right after the break and comparing with previous results the amount of void has increased reaching almost 0.35 in the cell number 89.

4.1.7 Results for pipe size 25m

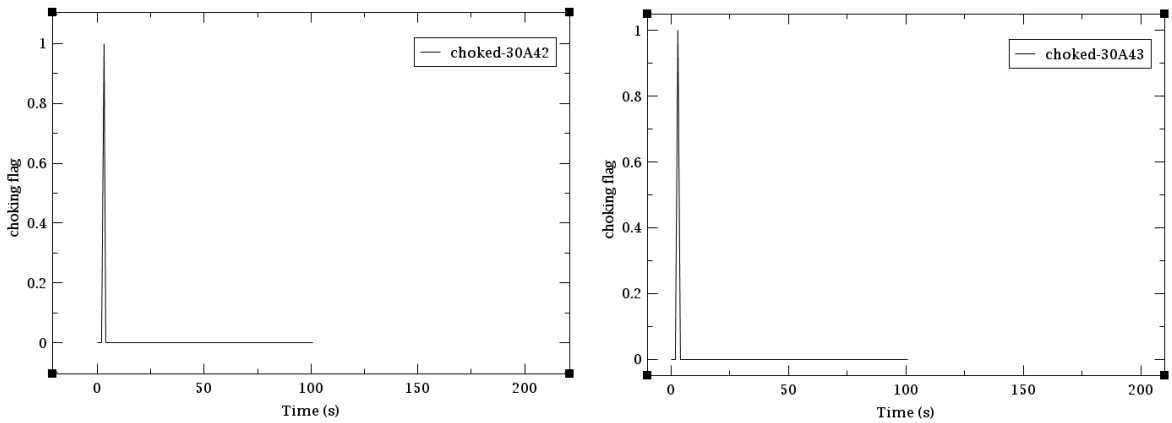

Figure 26. Graph of critical flow appearance of pressure 15.5 MPa, pipe size 25m on cell 42 and 43.

From the figure 26 it's possible to see the appearance of the critical flow phenomena in two cells, where the result showed that it appears right after the break in 2 seconds and doesn't last longer.

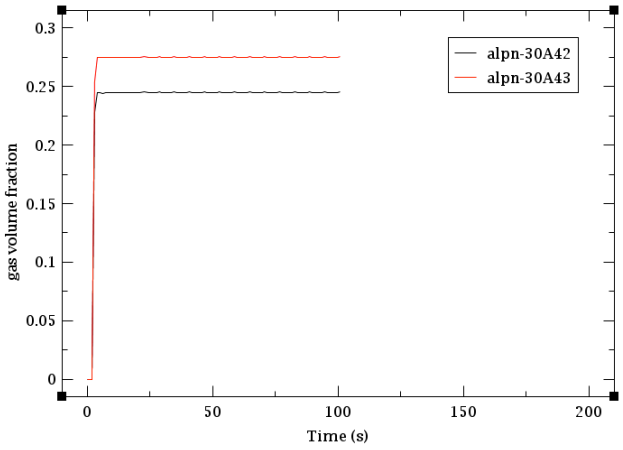

Figure 27. Graph of void fraction on Pressure 15.5 MPa, pipe size 25m.

From the result it's possible to see that the amount of void in both cells start increasing right after the break and it is less comparing with the previous result like 22.24m. The void appears and continue with no change.

4.2 Critical flow and void fraction for pressure 15MPa

Here will be presented the results for all the different pipe sizes with the same initial pressure 15MPa.

4.2.1 Results for pipe size 0,8 m

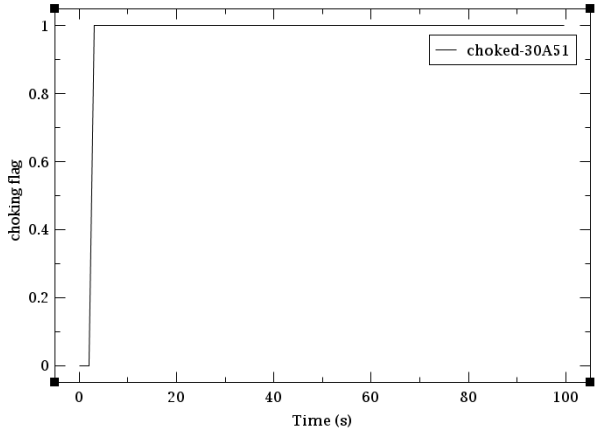

Figure 28. Graph of critical flow appearance of pressure 15MPa, pipe size 0.8m on cell 51.

It's possible to see from the result in the figure 28 that the critical flow phenomena appears in the cell 51, at the time 2 seconds right after the break and continues along the time.

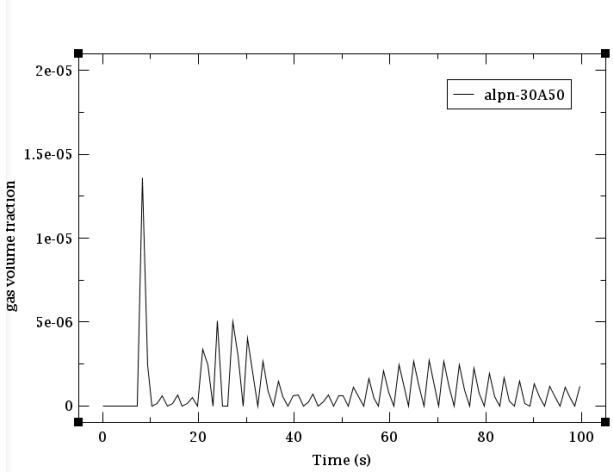

Figure 29. Graph of void fraction on pressure 15MPa, pipe size 0.8m.

Void has appeared in the last cell right after the break but as it can be seen from the figure 29 the scale is considered to be too small as void fraction has scale from 0 to 1.

4.2.2 Results for pipe size 5m

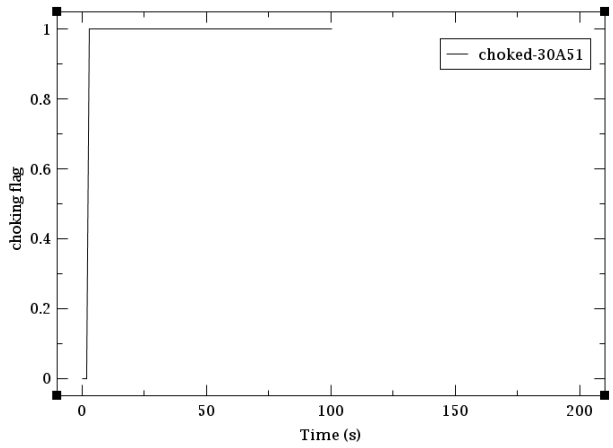

Figure 30. Graph of critical flow appearance of pressure 15 MPa, pipe size 5m on cell 51.

As it can be seen from the figure 30 the critical flow phenomena has appeared in the cell 51 and it has be continued along the time.

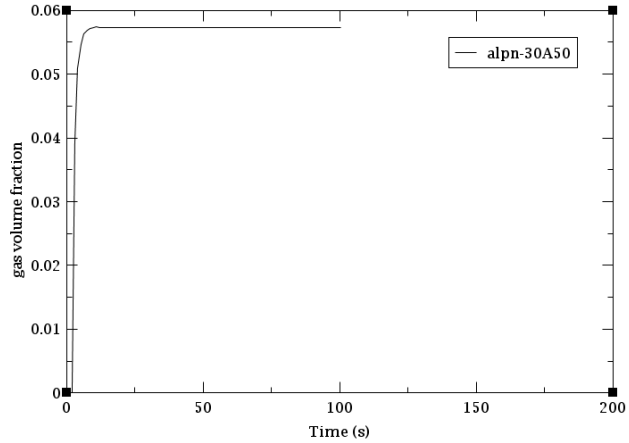

Figure 31. Graph of void fraction on pressure 15 MPa, pipe size 5 m.

As it can be seen from the figure 31 that some void has been formed in the cell 50 right after the break, but in scale 0 to 1 is has been considered too small the amount as it doesn't reach at least 0.1.

4.2.3 Results for pipe size 10m

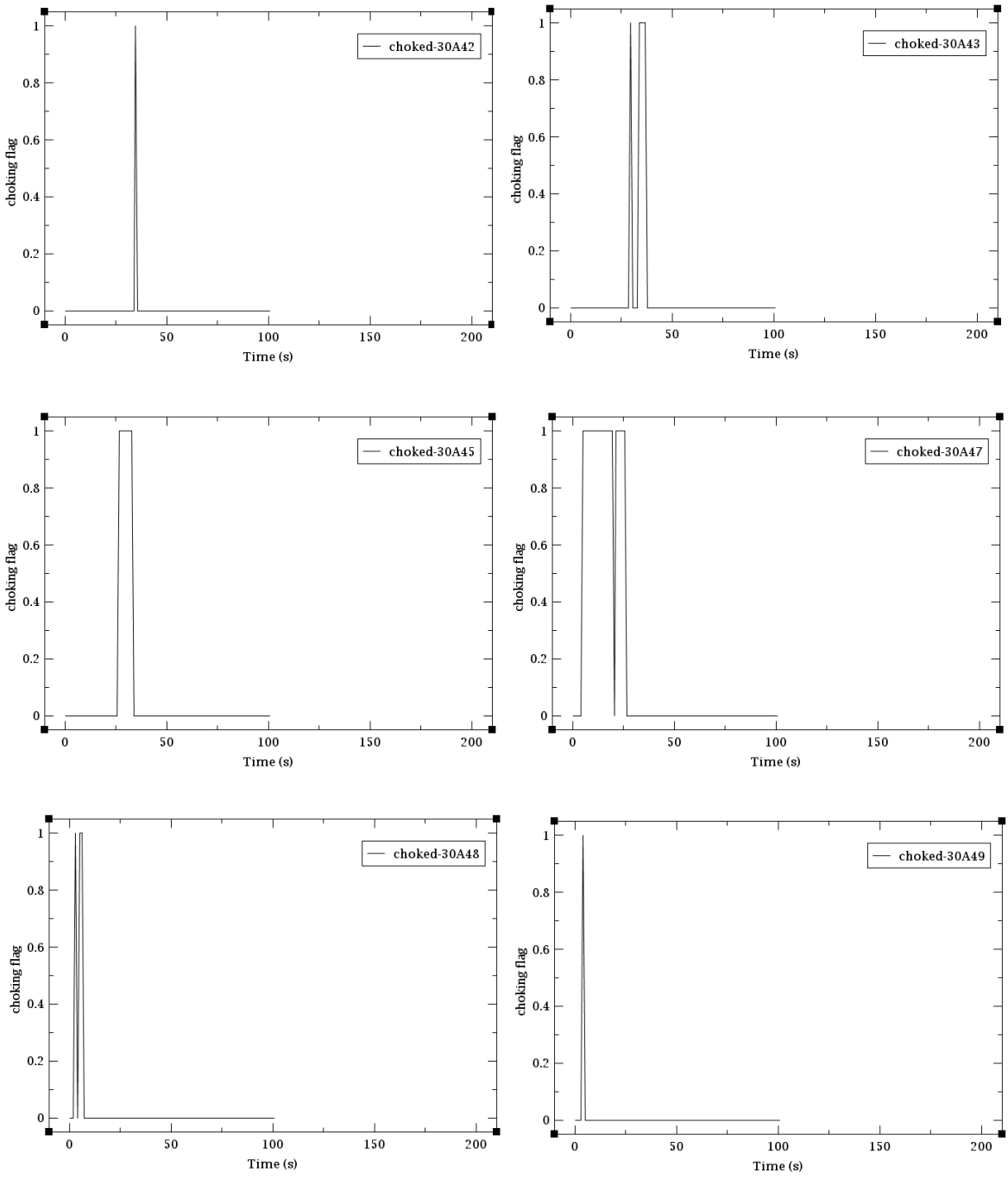

Figure 32. Graph of critical flow appearance of pressure 15MPa, pipe size 10m on cell 42, 43, 45, 47, 48 and 49.

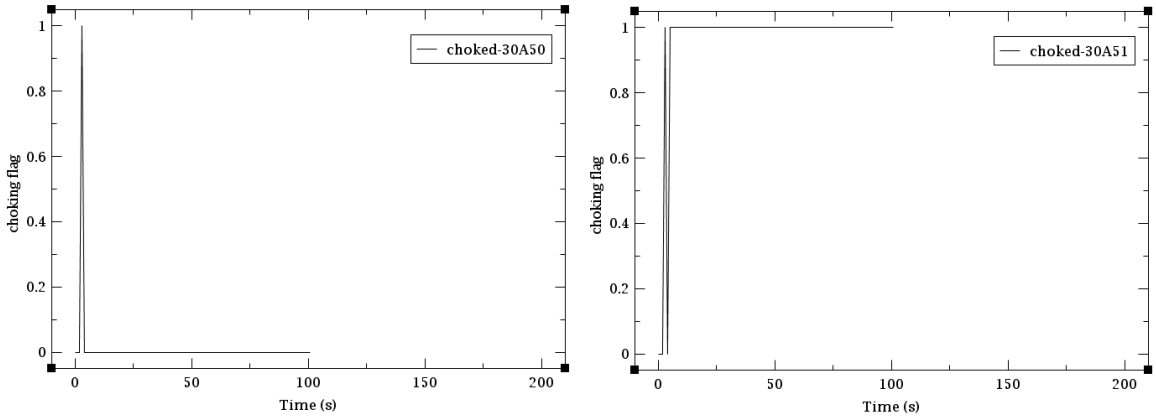

Figure 33. Graph of critical flow appearance of pressure 15MPa, pipe size 10m on cell 50 and 51.

As the result shows, we have the critical phenomena happening in more cell here than compared with the other sizes. On the cells 42, 43 and 45 we have some certain delay, when the break happens at the time 2 seconds, it takes some time to form the phenomena while the other cells we have the phenomena happening right after the break a quick formation with exception of cell number 51 that the phenomena continue to happen along the time.

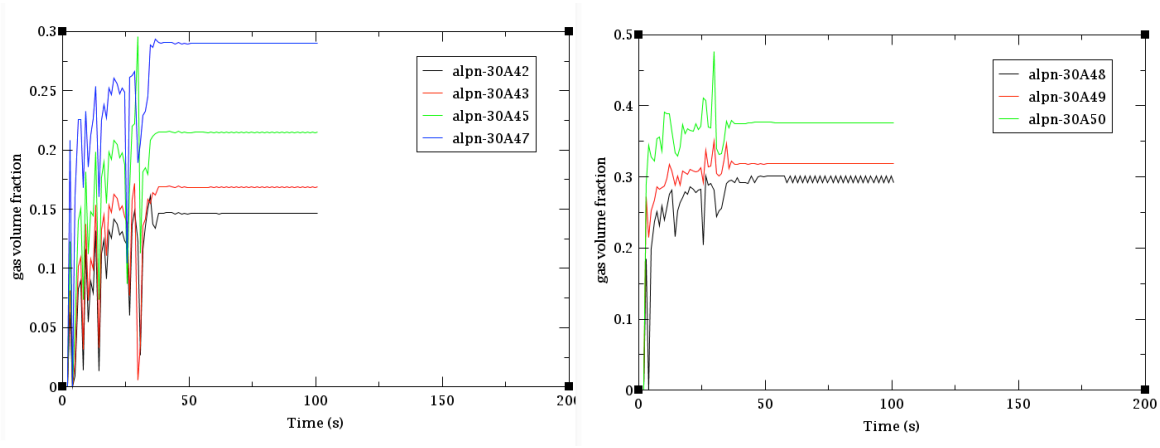

Figure 34. Graph of void fraction on Pressure 15 MPa, pipe size 10m.

It’s possible to notice from the figure 34 that we have a bit more formation of void in the cells where the critical flow phenomena appears in reflex of the phenomena itself and its possible to notice that the amount of void increase from one cell to the other.

4.2.4 Results for pipe size 15m

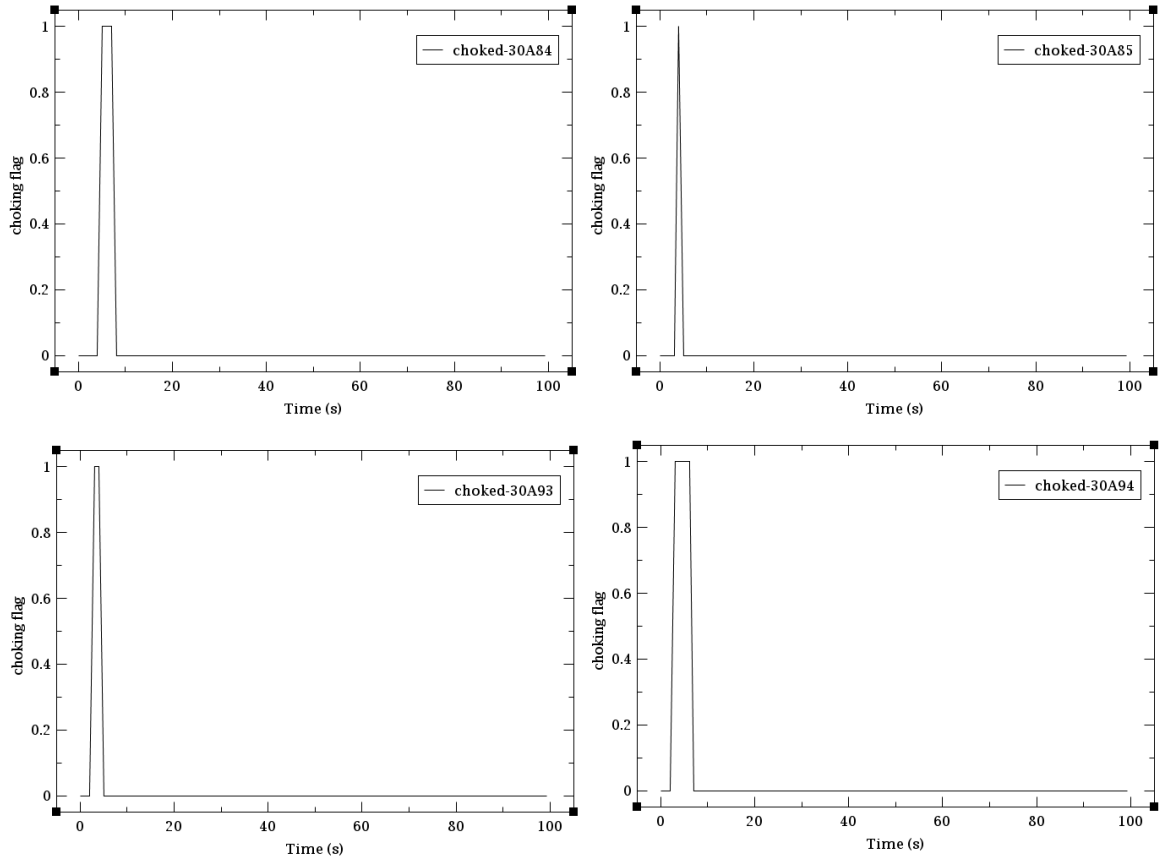

Figure 35. Graph of Critical Flow appearance of Pressure 15 MPa, pipe size 15m on cell 84, 85, 93 and 94.

Here is another example were by using 50 cells there were no possible to see the critical flow, so 100 cell had to be used in pro to see the results as the phenomena happens so fast.

The phenomena could only be seen to happen in the cells 84, 85, 93 and 94 and it seen to be a really fast phenomena as it appears right after the break at 2 seconds and doesn’t last longer during the modelling.

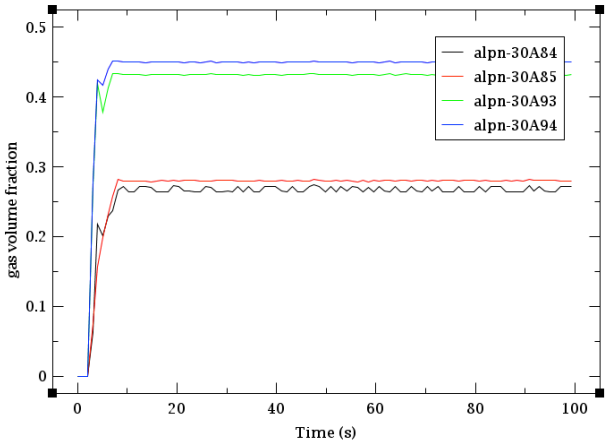

Figure 36. Graph of void fraction on pressure 15 MPa, pipe size 15m.

In this figure 36 it's possible to see that the amount of void has been formed right after the phenomena happens with a significant amount counted in the cell 94 and 93 from the previous results which has reached more than 0.4 in scale of 0 to 1.

4.2.5 Results for pipe size 20m

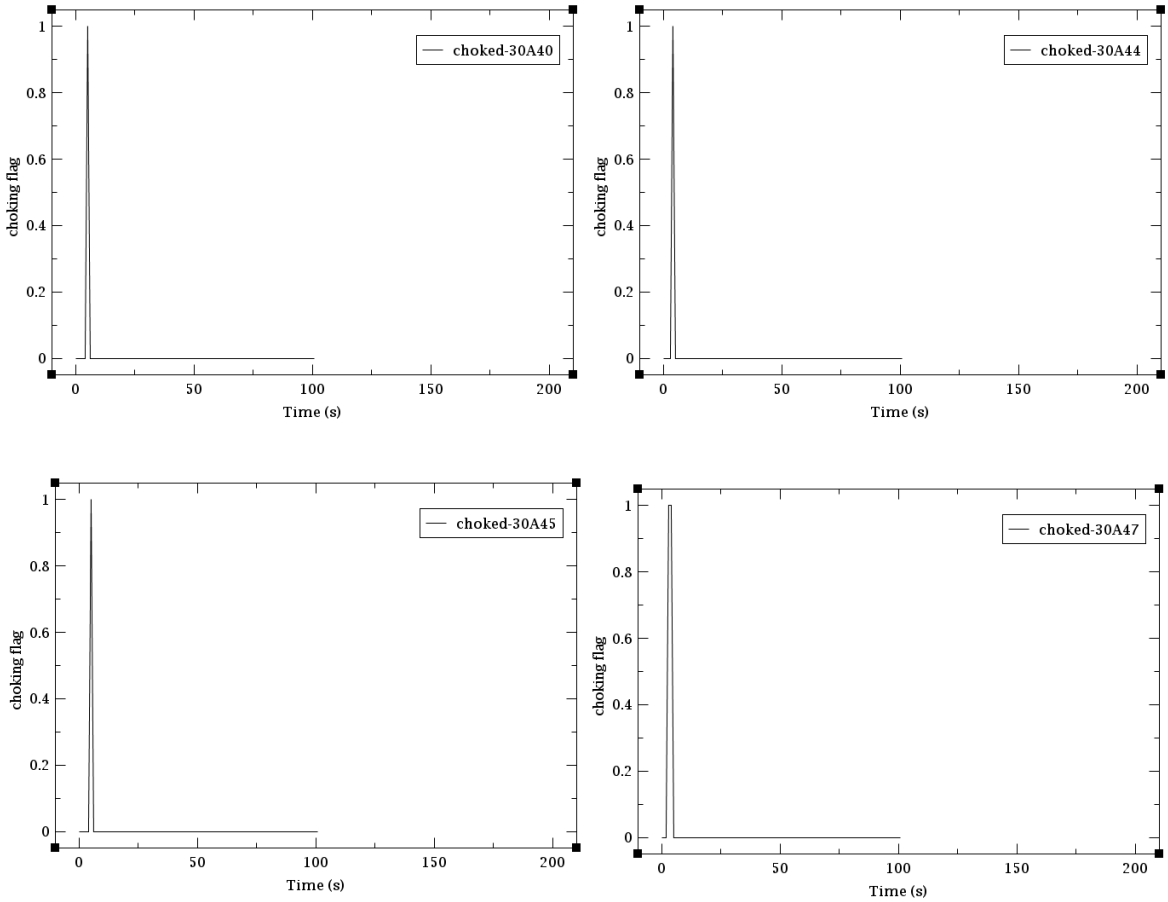

Figure 37. Graph of critical flow appearance of pressure 15 MPa, pipe size 20m on cell 40, 44, 45 and 47.

As it can be seen from the figure 37 the critical flow phenomena happens in 4 different cells right after the break happens and it doesn't last longer. We have a peak at the time 2 seconds but in the next second we can see no more critical flow.

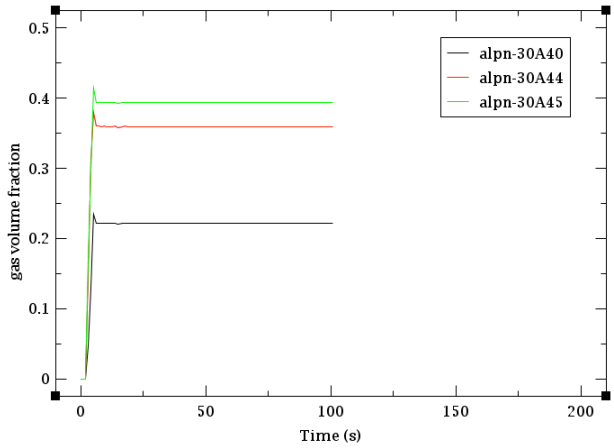

Figure 38. Graph of void fraction on pressure 15 MPa, pipe size 20m.

As it can be seen from the figure 38, significant amount of void has been formed in the cell where the critical flow has appeared right after the break happens, in the cell 40 goes to 0.21 in scale of 0 to 1, and the cell 44 and 45 more than 0.35 to 0.4.

4.2.6 Results for pipe size 22.24m

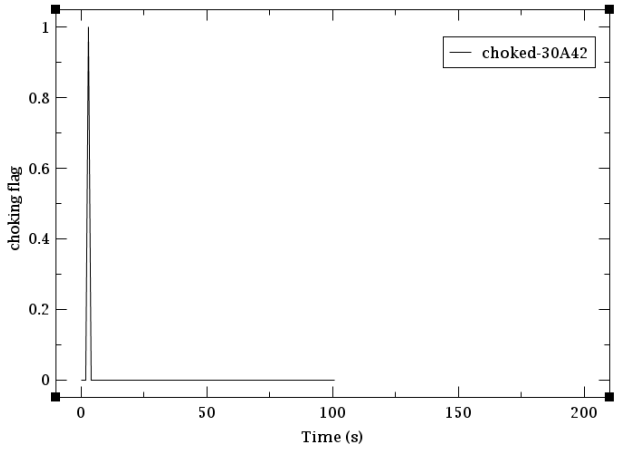

Figure 39. Graph of critical flow appearance of pressure 15MPa, pipe size 22.24 m on cell 42.

From the figure 39 it's possible to see that we have appearance only in one cell, and the critical flow phenomena in the cell 42 happens really fast and it doesn't last longer.

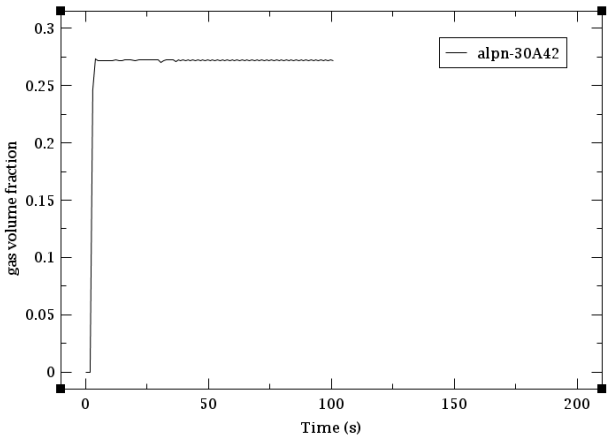

Figure 40. Graph of void fraction on pressure 15MPa, pipe size 22.24 m.

From the figure 40 it's possible to see to see that there is a formation of void in the cell where the critical flow phenomena happens of 0.28 in scale of 0 to 1.

4.2.7 Results for pipe size 25m

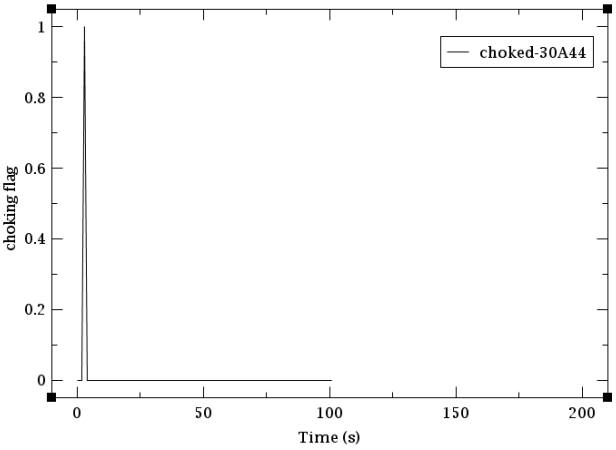

Figure 41. Graph of critical flow appearance of pressure 15 MPa, pipe size 25m on cell 44.

As it can be seen from the figure 41 the critical flow phenomena happens only in one cell right after the break happens and it doesn't last longer as only one peak appears and disappear right after.

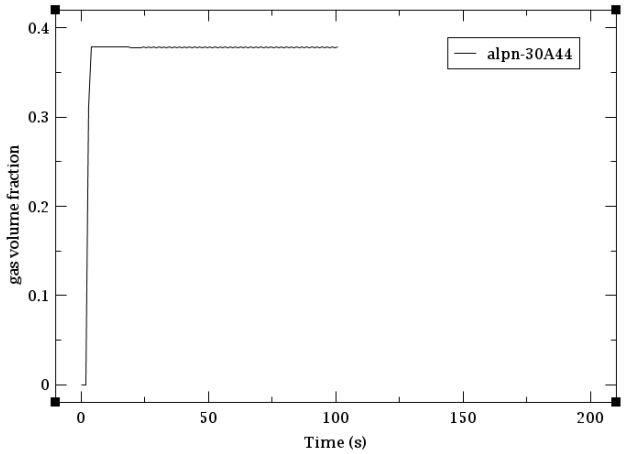

Figure 42. Graph of void fraction on pressure 15MPa, pipe size 25m.

There is a significant amount of void being formed right after the break happens at the time 2 seconds with amount of almost 0.4 in scale 0 to 1 different from the other values analyzed.

4.3 Critical flow and void fraction for pressure 14MPa

Here will be presented the results for all the different pipe sizes with the same initial pressure 14MPa.

4.3.1 Results for pipe size 0,8 m

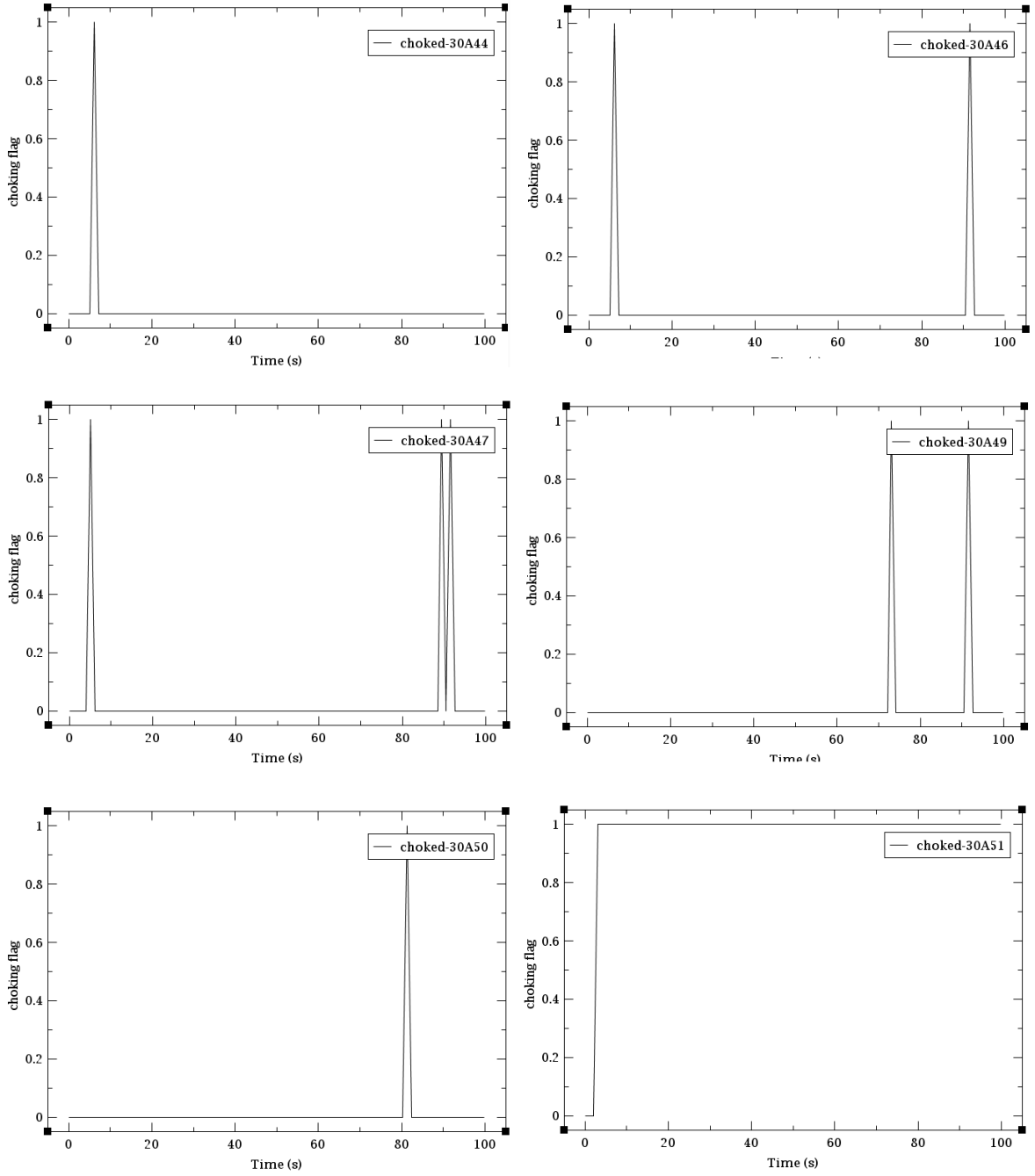

Figure 43. Graph of critical flow appearance of pressure 14MPa, pipe size 0.8m on cell 44, 46, 47, 49, 50 and 51.

From the figure 43 we can see the appearance of the phenomena critical flow on 6 different cells with behaviors that differs from each other, on the cell 44 and cell 51 we have the

choked flow happening right after the break at 2 seconds but the cell 51 the phenomena continue through the time. On the cells 46 and 47 the phenomena appears right after the break, disappear for a while and returns again, in the case of cell 46 we have one more peak at 90 seconds and cell 47 we have the appearance of the phenomena two more times almost at the end. On the cells 49 and 50 the phenomena showed a delay, nothing has happened when the break happened, but it appear later almost at the end of the time where cell 50 had only one peak noticed while cell 49 had 2 peaks.

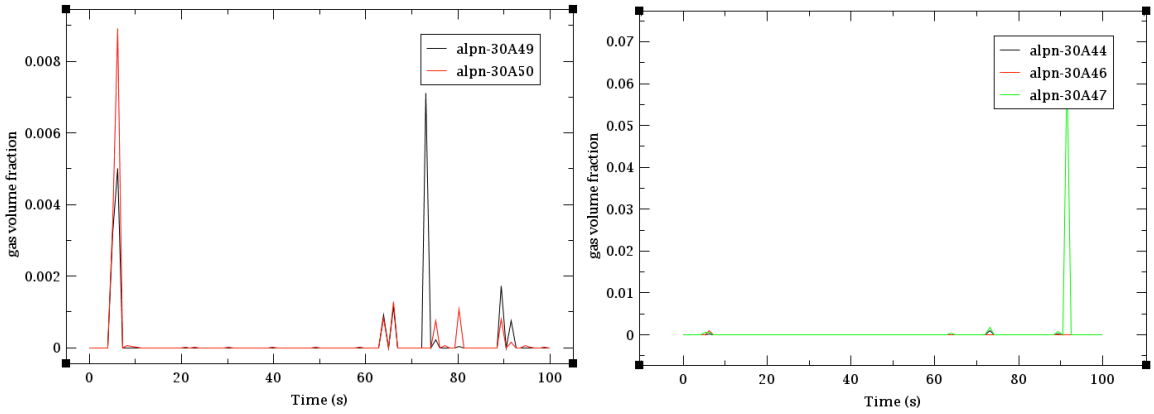

Figure 44. Graph of void fraction on pressure 14MPa, pipe size 0.8m.

From the figure 44 it's possible to noticed that a small amount of void has been formed where the critical flow phenomena appeared, we have on cell 49 and 50 that start void formation right after the break, but its considered to be too small as it doesn't reach 0.1 in scale of 0 to 1 used for void fraction, so the amount was minimal and on the cell 44, 46 and 47 the same, the amount was so small with exception of cell 47 where the void was formed with certain delay almost at the end of the time and also too small amount.

4.3.2 Results for pipe size 5m

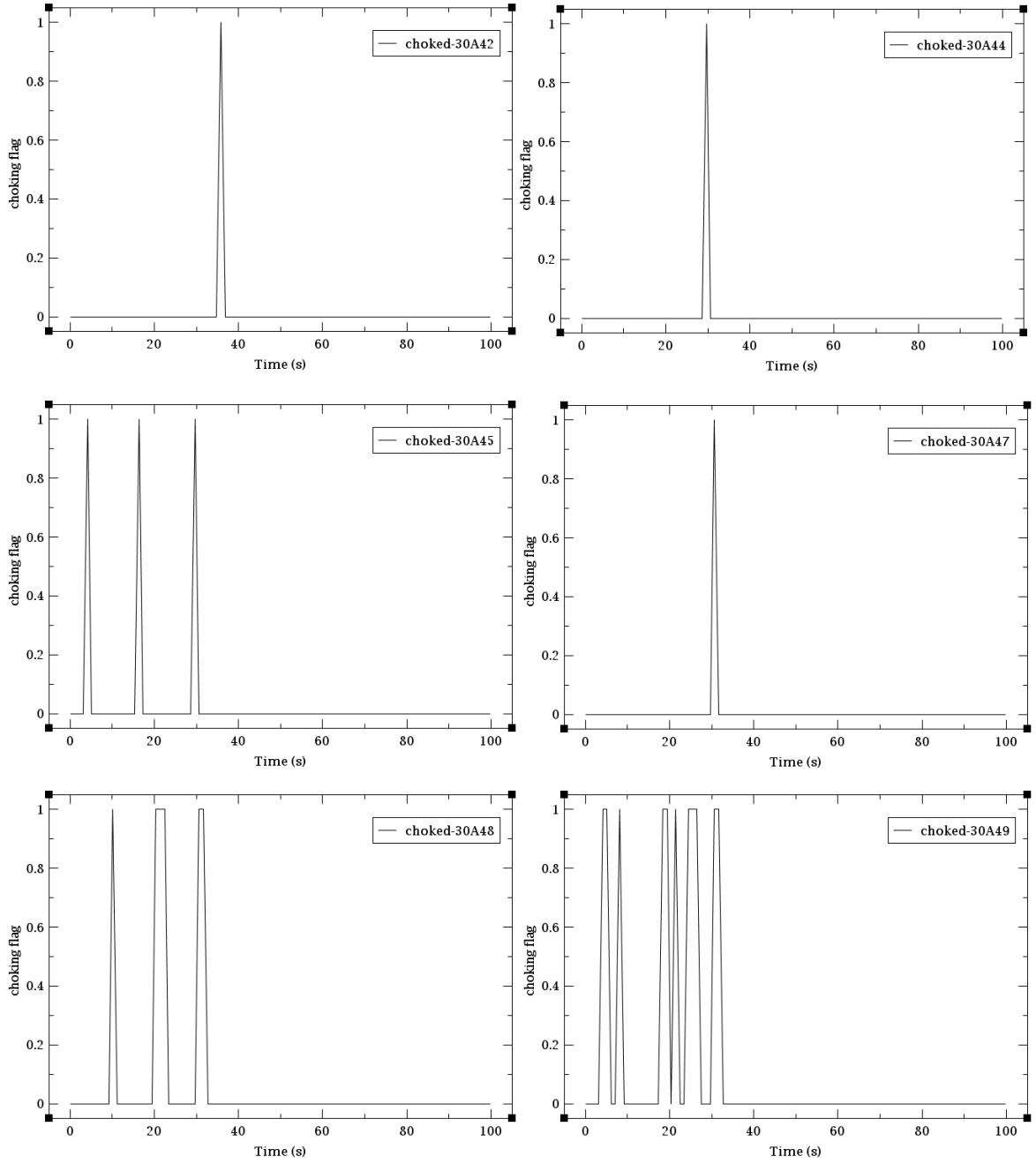

Figure 45. Graph of critical flow appearance of pressure 14MPa, pipe size 5m on cell 42, 44, 45, 47, 48 and 49.

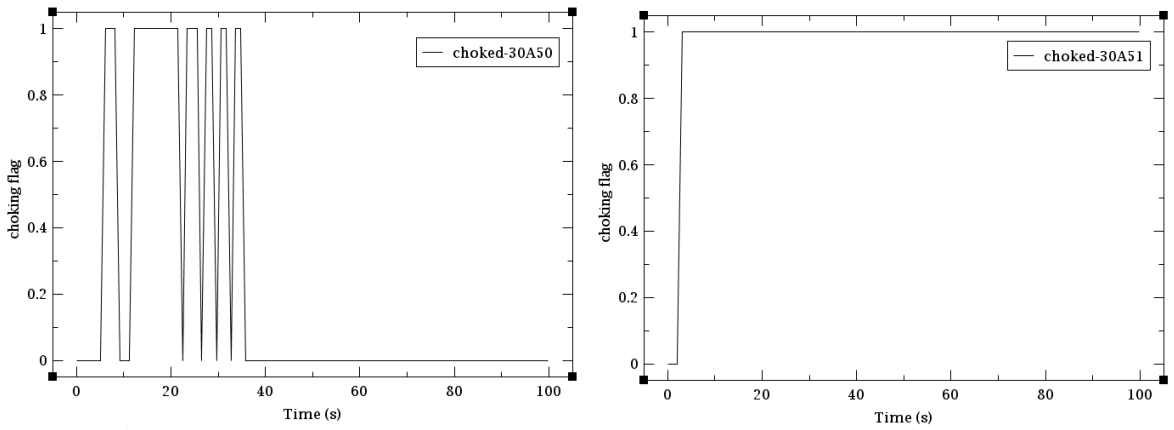

Figure 46. Graph of critical flow appearance of pressure 14MPa, pipe size 5m on cell 50 and 51.

From the figures 45 and 46 its possible to see the critical flow phenomena appearance in 8 different cells, so far has been the analyze which has the most critical flow appearance, in the figure 45 we can see cells 42, 44, 47 and 48 had some delay, the phenomena appears past 30 seconds of simulation, cells 45 and 49 the phenomena was right after the break at 2 seconds, but it has appeared again. Cell 49 had a different shape similar with cell number 50 from the figure 46 where the phenomena has lasted for some time, then disappear and that come back again while cell number 51 the phenomena happened right after the break and continued along the time.

Unfortunately, the results from void fraction in some modelling parts we not possible to obtain, and this case has been on of then.

4.3.3 Results for pipe size 10m

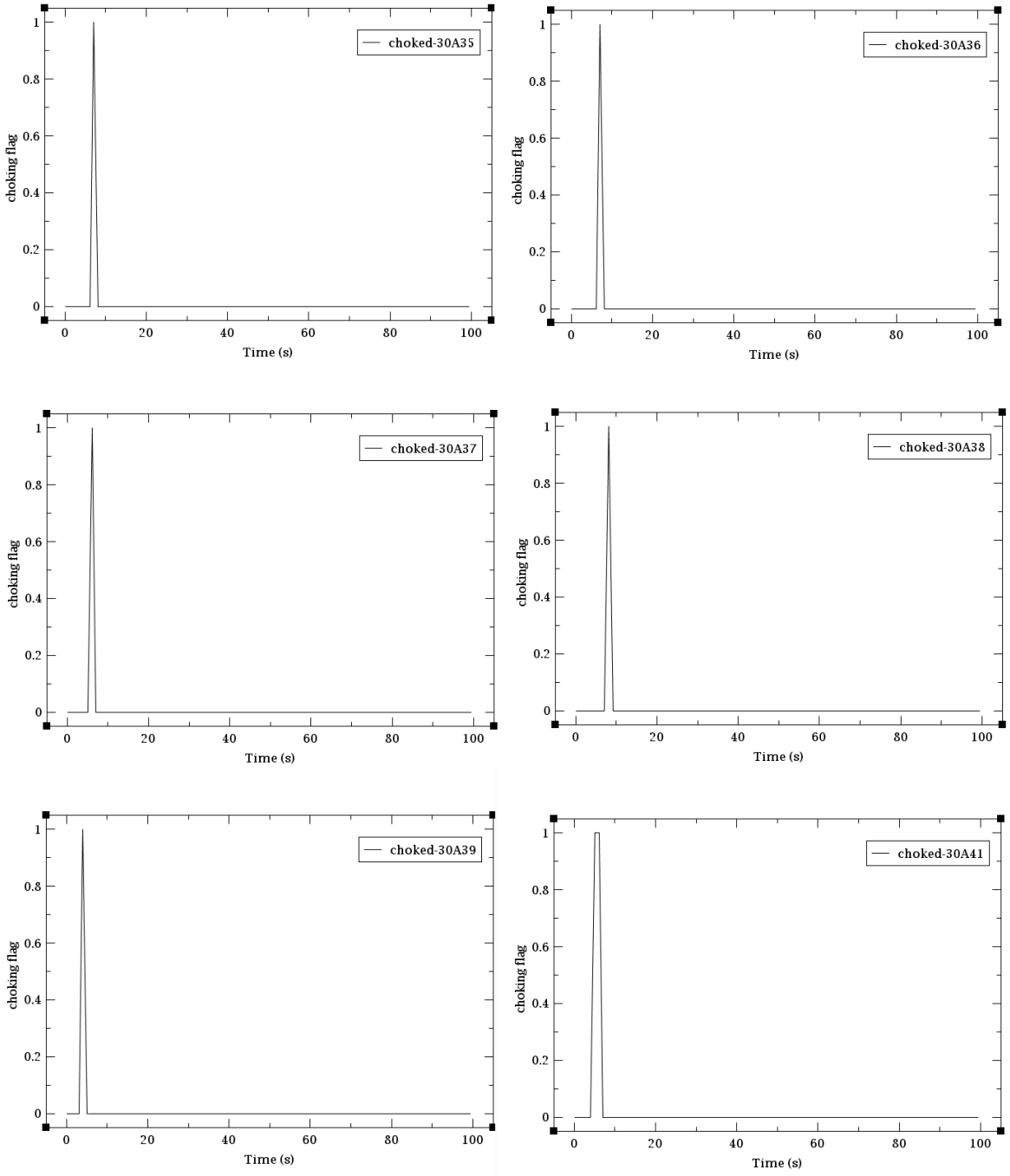

Figure 47. Graph of critical flow appearance of pressure 14MPa, pipe size 10m on cell 35, 36, 37, 38, 39 and 41.

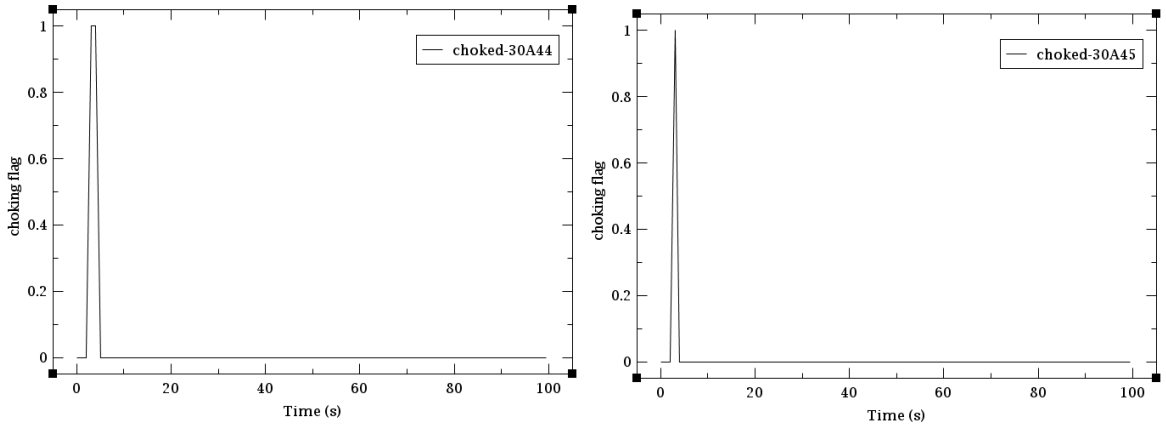

Figure 48. Graph of critical flow appearance of pressure 14MPa, pipe size 10m on cell 44 and 45.

As it can be seen from the figure 47 and 48, there was the appearance of the phenomena critical flow in 8 different cells with a similar shape where in all cases the event happens right after the break at 2 seconds, doesn't last longer with exception of cell 41 and 44 where it las lasted for 2 seconds before it disappear.

Here another example where the results for void fraction could not be found so unfortunately there will not be a result.

4.3.4 Results for pipe size 15m

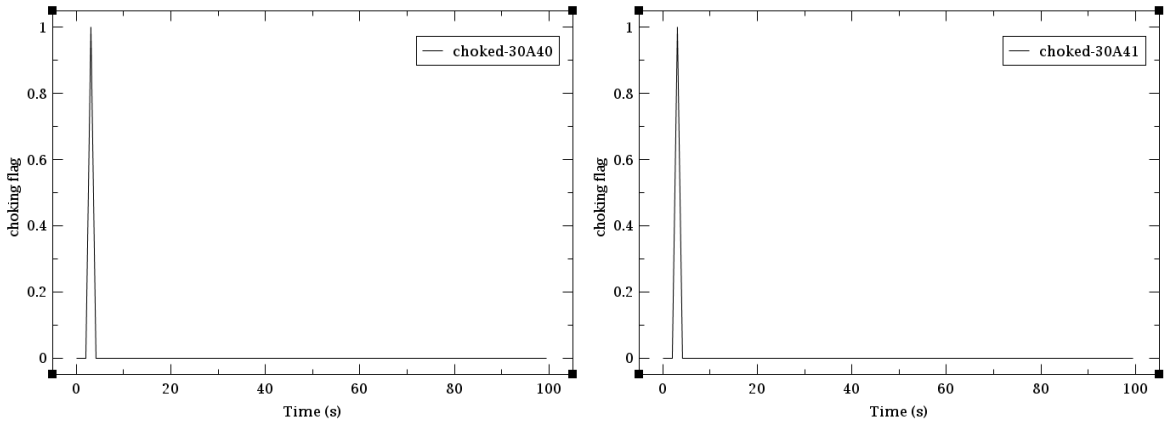

Figure 49. Graph of critical flow appearance of pressure 14MPa, pipe size 15m on cell 40 and 41.

In this case we can see from the figure 49 that we had only the appearance of critical flow phenomena in 2 cells, 40 and 41 where the phenomena were right after when the break happened at 2 seconds where the chocked flow didn't las longer.

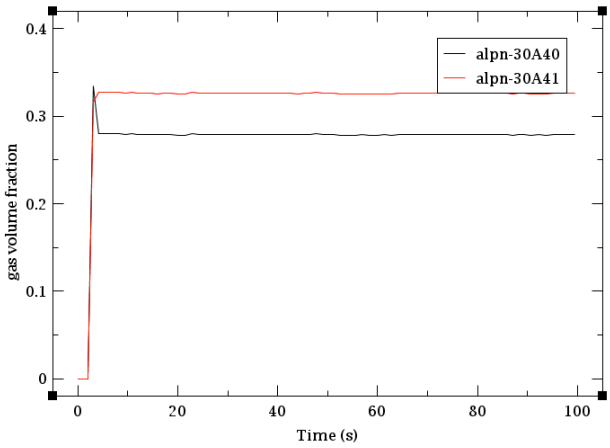

Figure 50. Graph of void fraction on pressure 14MPa, pipe size 15m.

From the figure 50 we can see a significant amount of void has been formed right after the break at 2 seconds of more than 0.3 in scale 0 to 1. The cell number 40 a few seconds after its formation, the amount has decreased a little and lasting during all the simulation like the cell 41.

4.3.5 Results for pipe size 20m

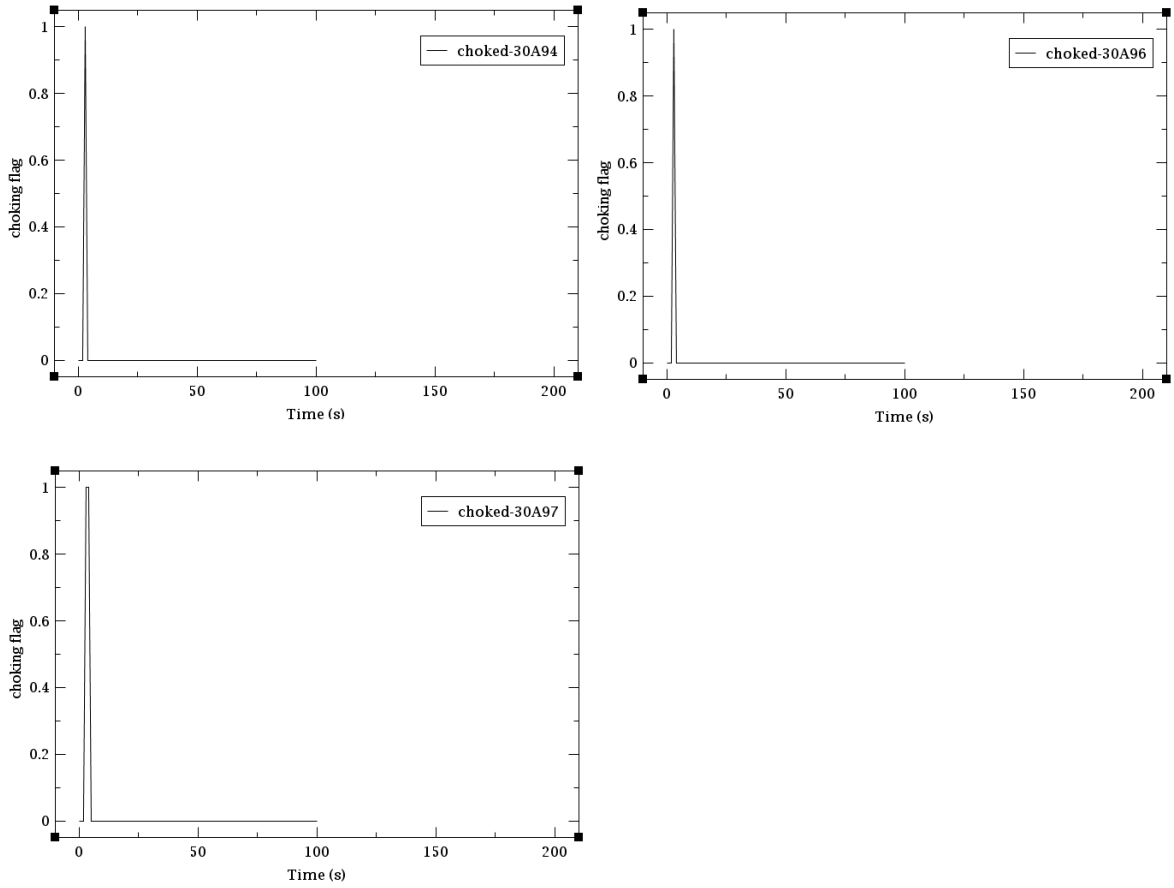

Figure 51. Graph of critical flow appearance of pressure 14MPa, pipe size 20m on cell 94, 96 and 97.

As mentioned before, as the phenomena happens too fast some cases were not possible to find the critical flow using only 50 cells, in this case we can see another example of how fast the phenomena happens, so it was not possible to see the critical flow only in 50 cells, so 100 cells had to be analysed in pro to be able to see.

We can see that the phenomena have happened in 3 different cells and having the same shape, the critical flow appears right after the break at 2 seconds but doesn't last longer, just one peak in all three cells.

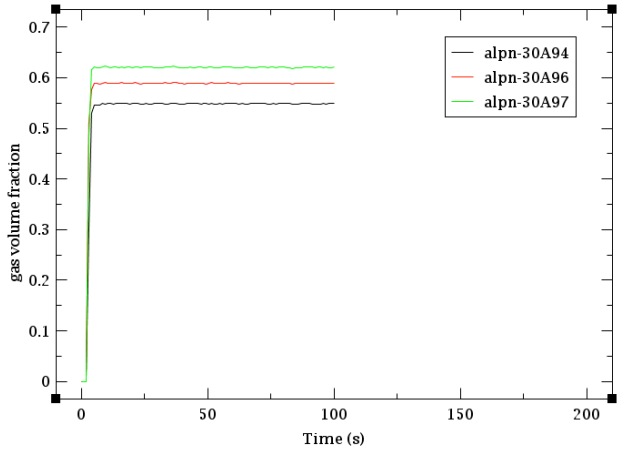

Figure 52. Graph of void fraction on pressure 14MPa, pipe size 20m.

From the figure 52 we can see that there was a bigger formation of void in the cells where the critical flow phenomena has happened and more than 0.6 as in the case of cell number 97 in scale 0 to 1 is considered high.

4.3.6 Results for pipe size 22.24m

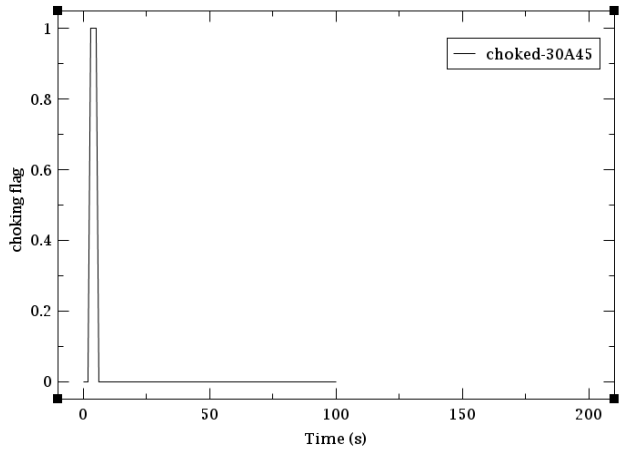

Figure 53. Graph of critical flow appearance of pressure 14MPa, pipe size 22.24m on cell 45.

As it can be seen from the figure 53 only one case of critical flow phenomena has happened right after the break, it has showed only one peak that lasted for a second.

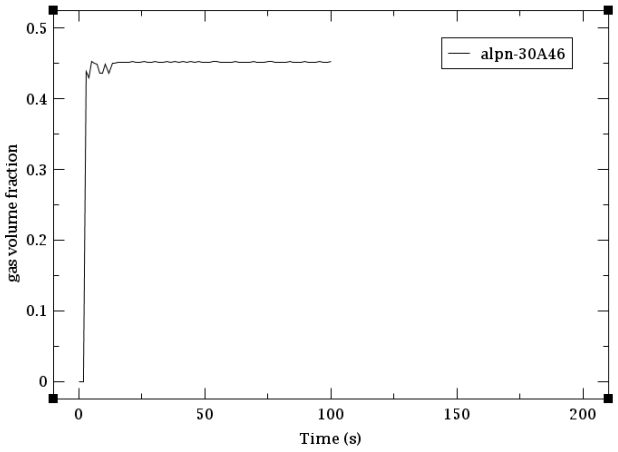

Figure 54. Graph of void fraction on pressure 14MPa, pipe size 22.24 m.

As it can be seen from the figure 54, a significant amount of void has been formed right after the break of 0.45 in scale of 0 to 1 and it has lasted during all the simulation.

4.3.7 Results for pipe size 25m

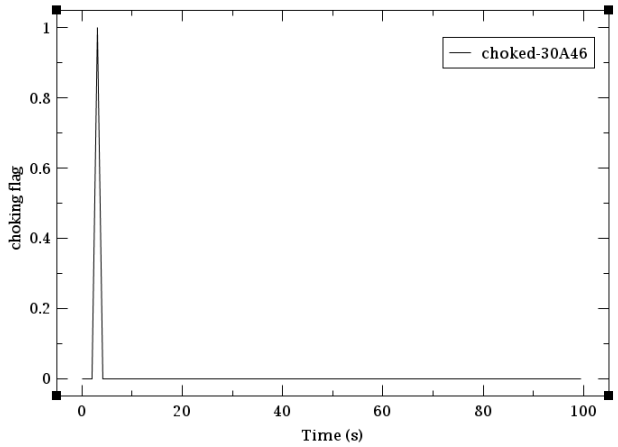

Figure 55. Graph of critical flow appearance of pressure 14MPa, pipe size 25m on cell 46

As it can be seen from the figure 55, the critical flow phenomena has appeared only in one cell right after the break and it didn't last longer, there was the formation and then disappear.

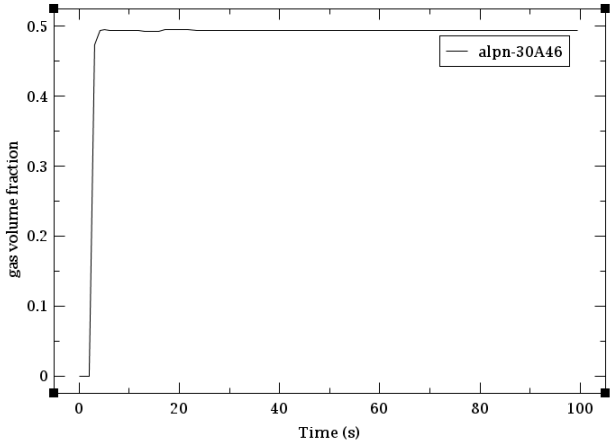

Figure 56. Graph of void fraction on pressure 14MPa, pipe size 25m.

A significant amount of void has been formed in the cell where the critical flow phenomena has appeared, 0.5 in scale of 0 to 1 and has continued with no change during all the simulation.

4.4 Critical flow and void fraction for pressure 13MPa

Here will be presented the results for all the different pipe sizes with the same initial pressure 13MPa.

4.4.1 Results for pipe size 0,8 m

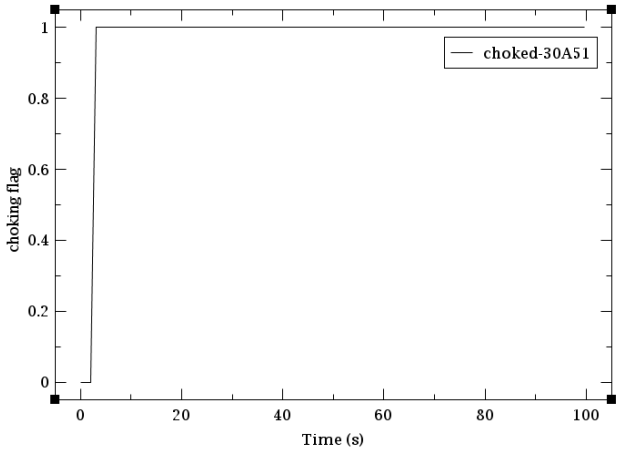

Figure 57. Graph of critical flow appearance of pressure 13MPa, pipe size 0.8 m on cell 51.

As it can be seen from the figure 57, the critical flow phenomena has appeared only in one cell right after the break and it has lasted during all the simulation.

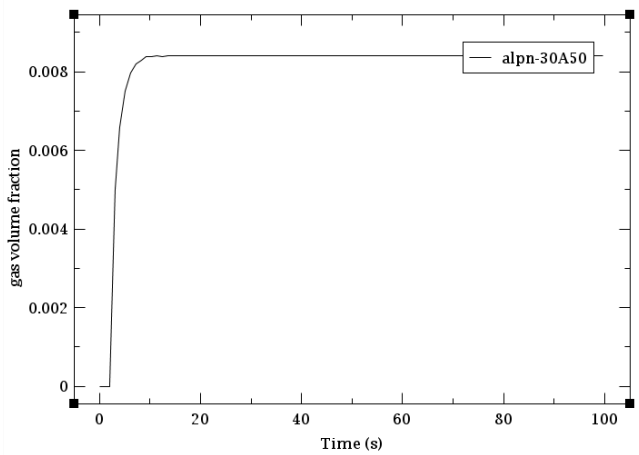

Figure 58. Graph of void fraction on pressure 13 MPa, pipe size 0.8m.

As it can be seen from the figure 58, some void has started to form right after the break at 2 seconds, but too small to be considered significant as it didn't reach 0.1.

4.4.2 Results for pipe size 5m

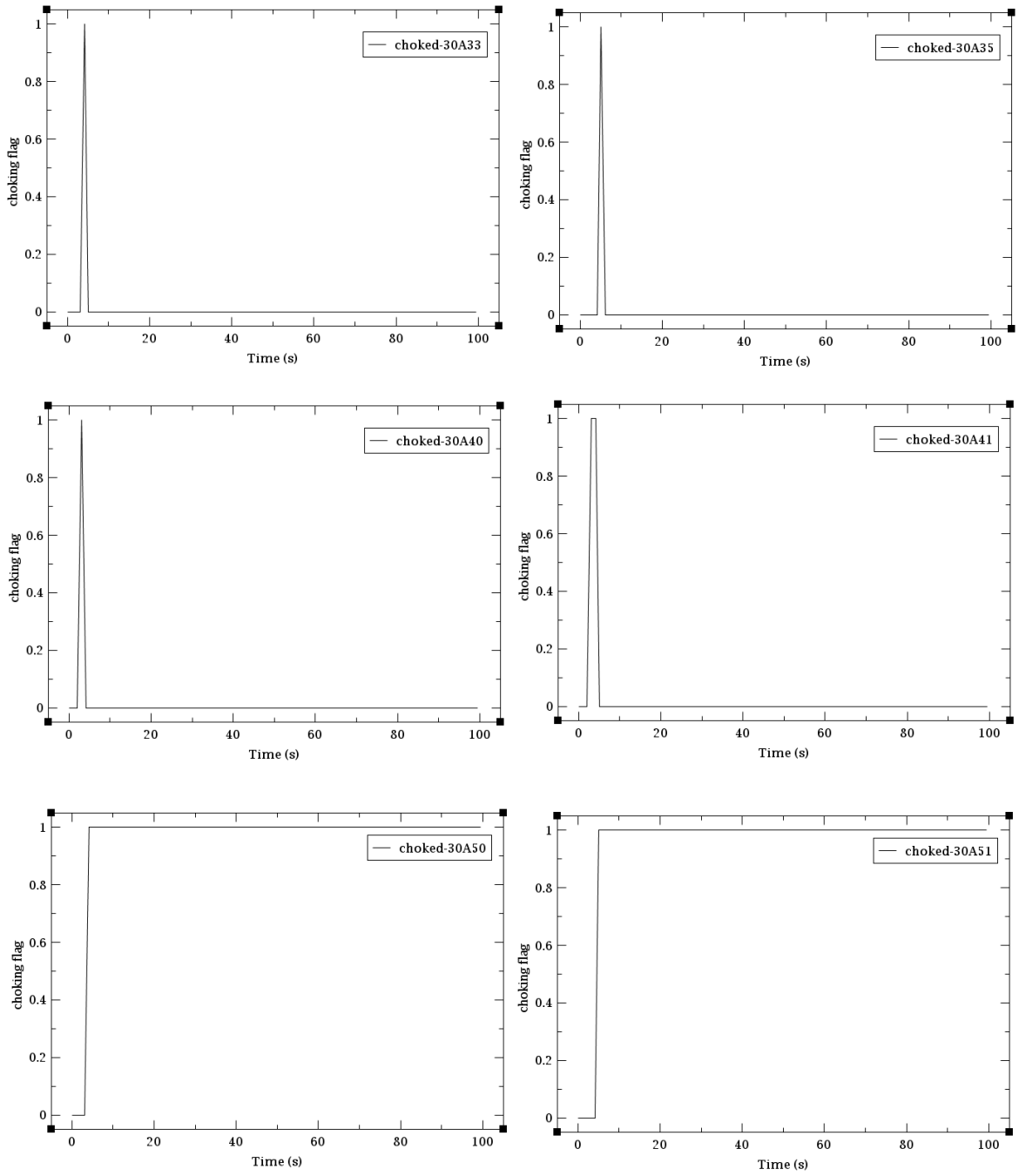

Figure 59. Graph of critical flow appearance of pressure 13MPa, pipe size 5m on cell 33, 35, 40, 41, 50 and 51.

As it can be seen from the figure 59, in this case the critical flow phenomena has appeared in 6 different cells where in the cells 33, 35, 40 and 41 there was only one peak right after

the break while in the cells 50 and 51 the phenomena also happens right after the break but it last during all the simulation.

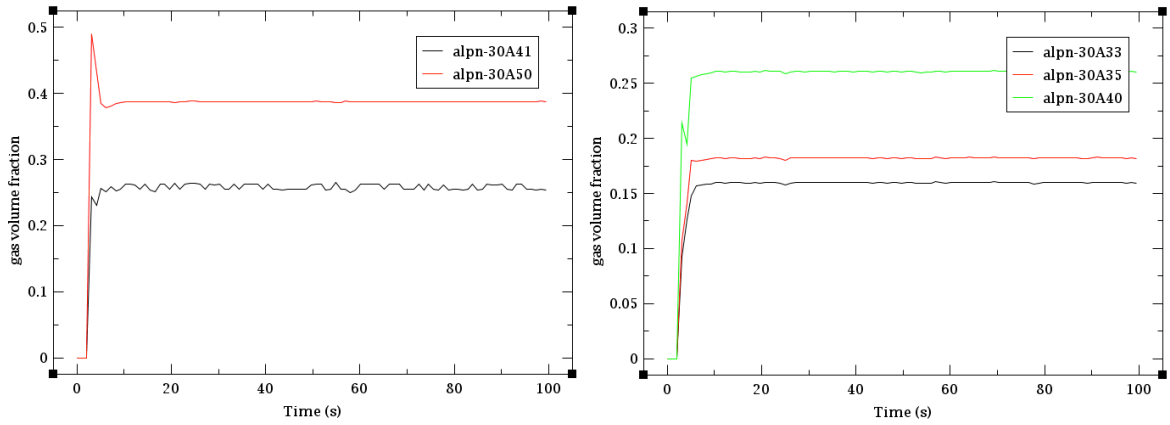

Figure 60. Graph of void fraction on pressure 13MPa, pipe size 5m.

As it can be seen from the figure 60, there was a significant amount of void been formed in the cells where the critical flow phenomena appeared right after the break happens. Cell 50 has almost reached 0.5 and in seconds decreased to 0.4 that has lasted this way along the time, cells 40 and 40 has formed 0.25 that oscillates during the time while cells 40 and 35 there is a little oscillation during the time, but it has continued constant along the time.

4.4.3 Results for pipe size 10m

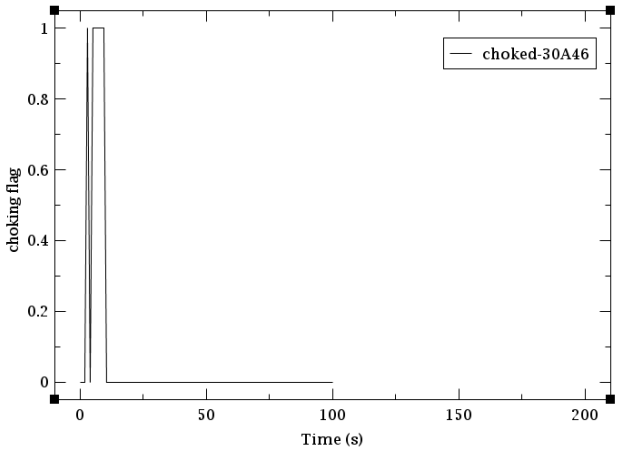

Figure 61 Graph of critical flow appearance of pressure 13 MPa, pipe size 10m on cell 46.

As it can be seen from the figure 61, we have only one case where the critical flow phenomena has happened right after the break at 2 seconds with 2 peak one coming right after the other that doesn't last longer.

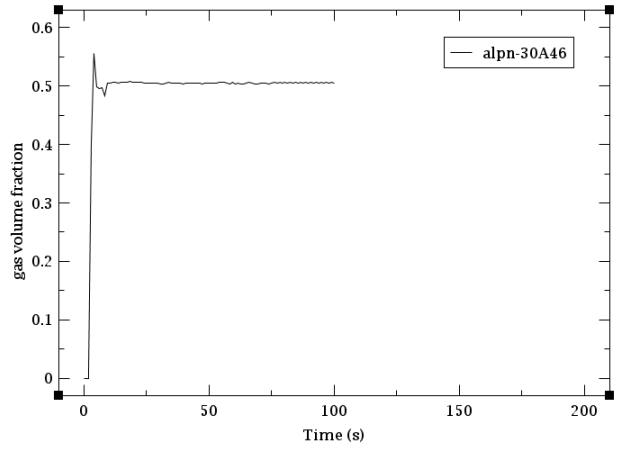

Figure 62. Graph of void fraction on pressure 13 MPa, pipe size 10m.

As it can be seen from the figure 62, a significant amount of void has been formed in the cell where the critical flow phenomena has happened right after the break at 2 seconds reaching

the peak of 0.55 in scale 0 to 1 than decreasing to 0.5 and continuing constant during the simulation.

4.4.4 Results for pipe size 15m

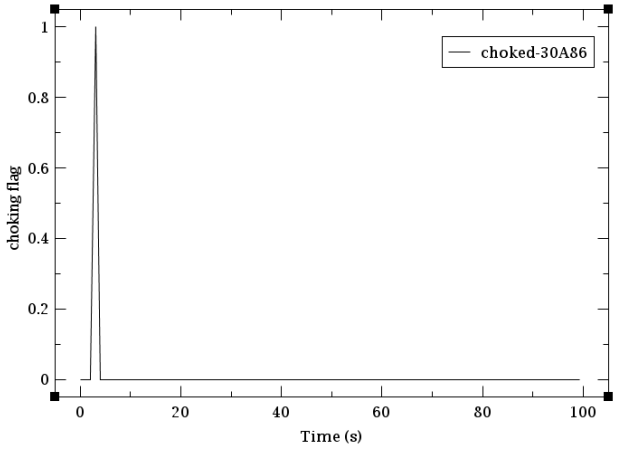

Figure 63. Graph of critical flow appearance of pressure 13MPa, pipe size 15m on cell 86.

As mentioned before, as the phenomena happens too fast some cases were not possible to find the critical flow using only 50 cells, here is another example of when it was not possible to see the critical flow only by using 50 cells, so 100 cells needed to be used in pro to be able to see the phenomena.

As it can be seen from the figure 63, even using a large number of cells the phenomena has appeared only in one cell right after the break at 2 seconds with only one peak.

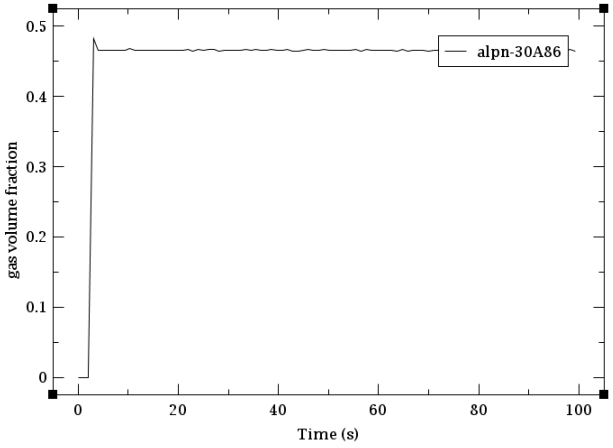

Figure 64. Graph of void fraction on pressure 13MPa, pipe size 15m.

As it can be seen from the figure 64, a significant amount of void has been formed right after the break at 2 second of 0.48 quick decreasing to 0.46 in scale of 0 to 1 and remaining constant during the simulation.

4.4.5 Results for pipe size 20m

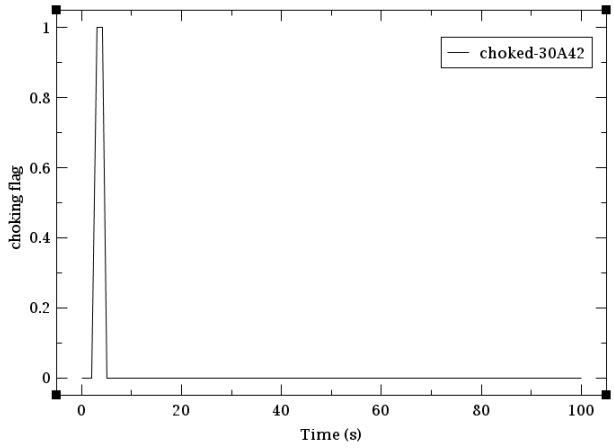

Figure 65. Graph of critical flow appearance of pressure 13MPa, pipe size 20m on cell 42.

As it can be seen from the figure 65, only one cell has showed the appearance of critical flow phenomena right after the break happens at 2 seconds that lasted for 2 seconds and then disappeared.

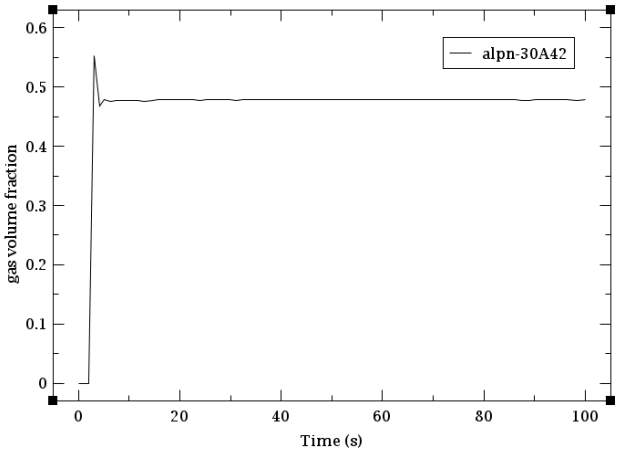

Figure 66. Graph of void fraction on pressure 13MPa, pipe size 20m.

As can be seen from the figure 66, a significant amount of void has been formed right after the break at 2 seconds in the cell where the critical flow phenomena has appeared of 0.5 than decreasing to 0.47 in scale of 0 to 1 and remaining constant during the simulation with no changes.

4.4.6 Results for pipe size 22.24m

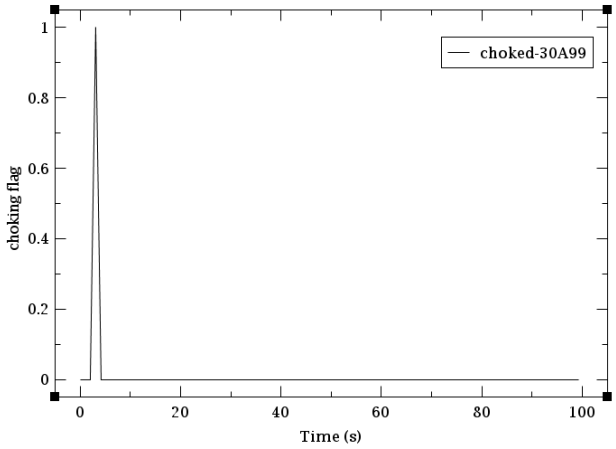

Figure 67. Graph of critical flow appearance of pressure 13 MPa, pipe size 22.24m on cell 99.

As mentioned before, as the phenomena happens too fast some cases were not possible to find the critical flow using only 50 cells, so here we have an atypical example for this experiment. As mentioned before that the phenomena happens so fast, some cases it was needed to increase the number of cells from 50 to 100 so it could be able to see the critical flow, but in this specific case, only 100 was not possible, so it was needed to increase to 150 cells, so the results below are from 150 cells.

So, as it can be seen from the figure 67, even increasing the amount of cell to be analyzed the critical flow phenomena could be identified only in cell with only one peak right after the break happens at 2 seconds.

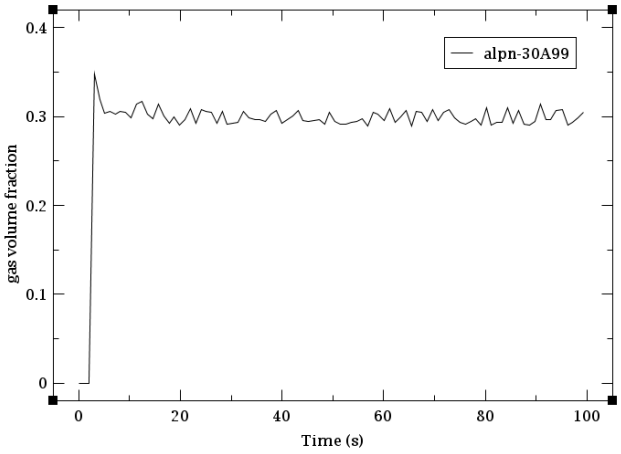

Figure 68. Graph of void fraction on pressure 13MPa, pipe size 22.24m.

As it can be seen from the figure 68, an amount of void has been formed in the cell 99 where the critical flow phenomena have happened right after the break happens at 2 second reaching a peak of 0.35 in scale of 0 to 1 soon decreasing to 0.3 where it has oscillating during the rest of the simulation.

4.4.7 Results for pipe size 25m

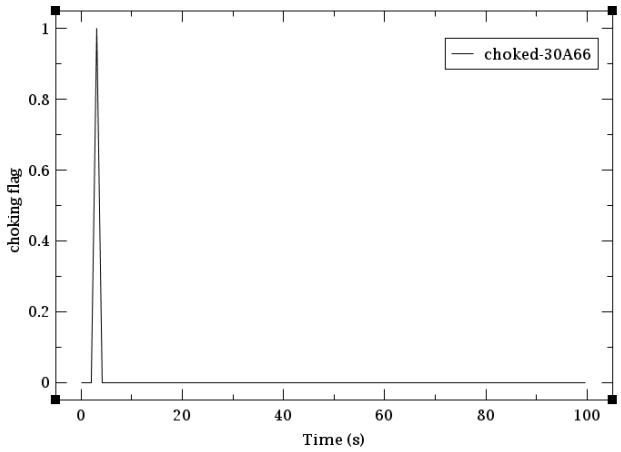

Figure 69. Graph of critical flow appearance of pressure 13MPa, pipe size 25m on cell 66.

As mentioned before, as the phenomena happens too fast some cases were not possible to find the critical flow using only 50 cells, so this case is also one of the examples when it was not possible to see the phenomena critical flow by only using 50 cells, so 100 cells were needed in pro to be able to see and obtain the result.

As it can be seen from the figure 69, only one cell has shown the appearance of the critical flow phenomena right after the break happens at time 2 seconds and didn't last longer.

4.5 Summary Results

Table 3. Total mass flow rate for different length and pressure configuration

Length, m	Primary pressure, MPa			
	15.50	15.00	14.00	13.00
	Total mass flow rate, kg/s			
0.8	21.60	19.65	14.98	10.33
5.00	9.77	9.29	8.38	7.35
10.00	7.74	7.59	6.73	5.30
15.00	6.63	6.23	5.41	4.42
20.00	5.68	5.35	4.60	3.89
22.24	5.37	5.06	4.38	3.69
25.00	5.05	4.75	4.13	3.45

Table 3 shows a clear dependency of the mass flow rate increase with increasing primary pressure. Conversely, an increase in pipe length results in a decrease in mass flow rate. This fact can be attributed to the turbulence generated by the turbulent flow, and the longer the pipe length, the more it hinders the flow of liquid.

A graphical representation of the transition point from single-phase fluid to two-phase two-component flow is the most obvious from the point of view of choked flow definition. Figures 70-76 below show comparative plots of the vapor fraction along the pipe for a steady state flow after 70 seconds from the start of the experiment. Each of the figures is

characterized by a certain pipe length but at different primary pressure, where blue line corresponds to 15.5 MPa, green line to 15 MPa, red line to 14 MPa and black line to 13 MPa.

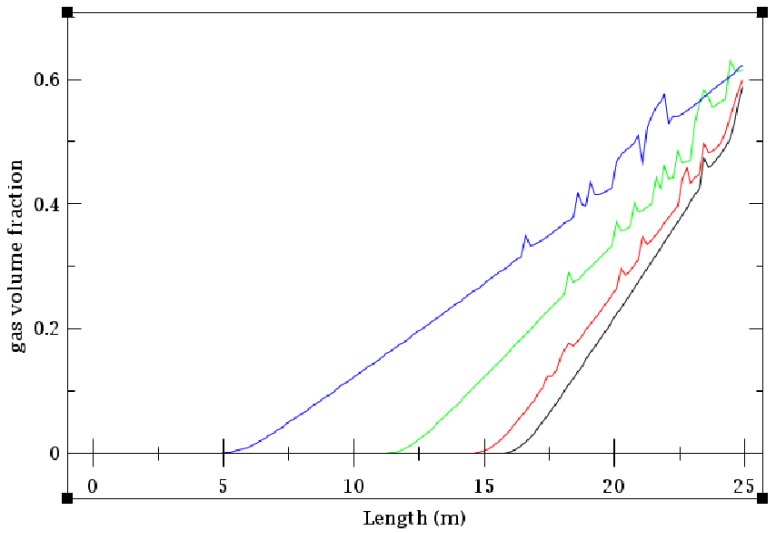

Figure 70. Void fraction along 25 m pipe for different primary pressures.

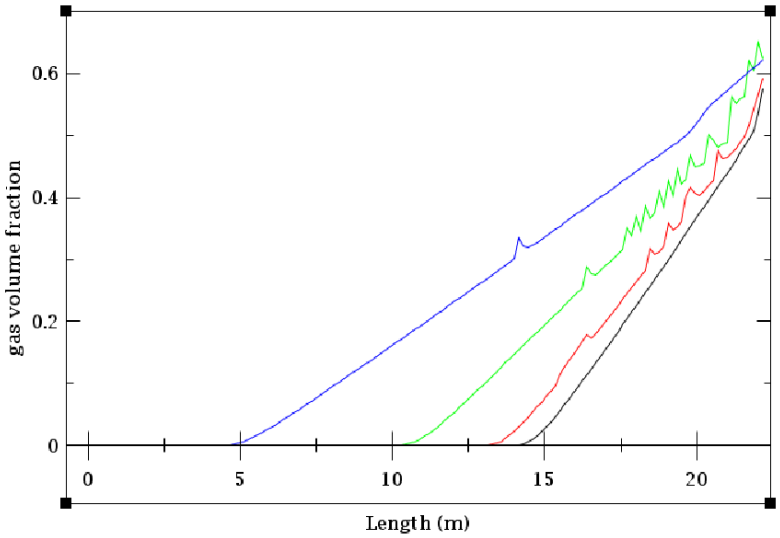

Figure 71. Void fraction along 22.24 m pipe for different primary pressures

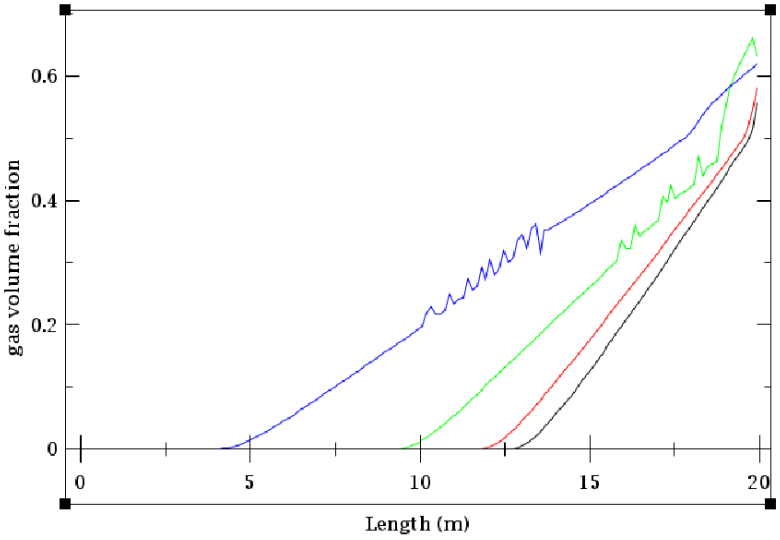

Figure 72. Void fraction along 20 m pipe for different primary pressures.

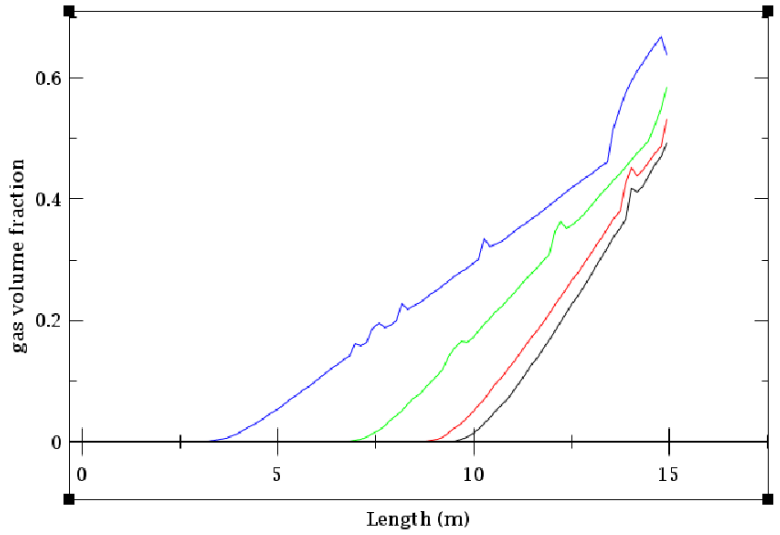

Figure 73. Void fraction along 15 m pipe for different primary pressures

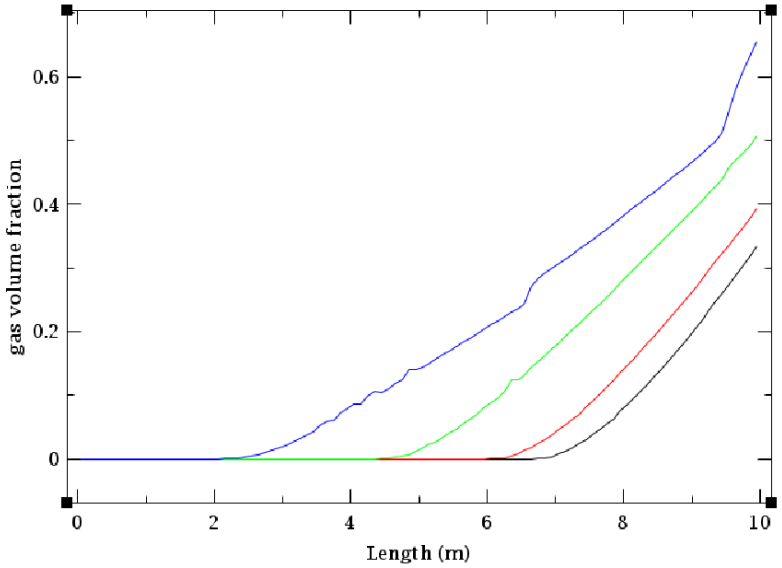

Figure 74. Void fraction along 10 m pipe for different primary pressures

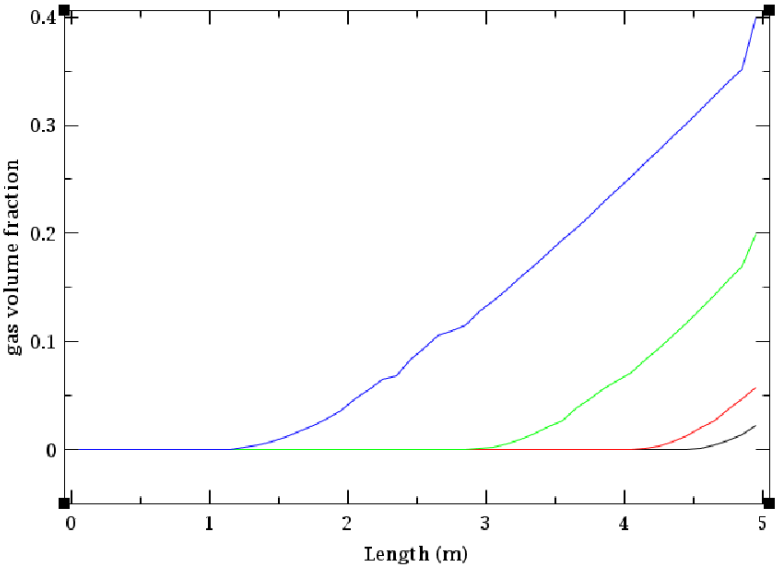

Figure 75. Void fraction along 5 m pipe for different primary pressures

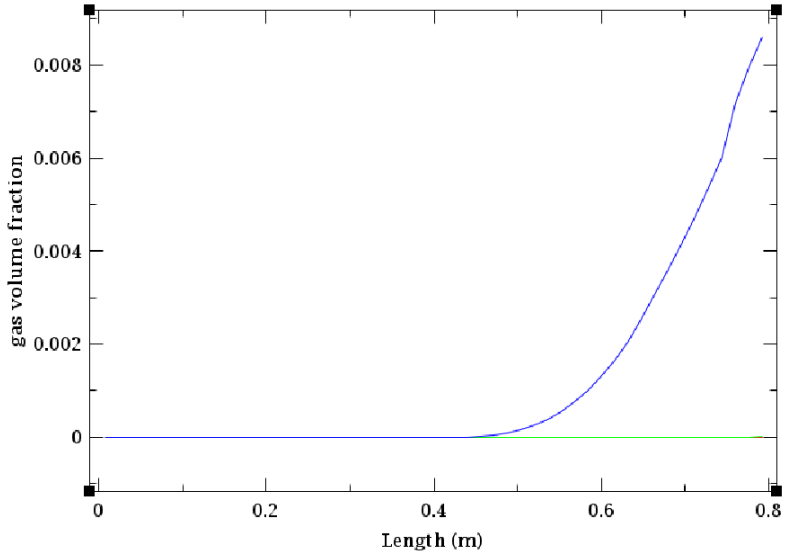

Figure 76. Void fraction along 0.8 m pipe for different primary pressures

As can be seen from the graphs above, their patterns are similar across the spectrum of pipe lengths from 5 to 25 meters. At a pressure of 15.5 MPa, gas bubble formation starts at approximately 1/5 of the pipe length. When the initial pressure is reduced by 0.5 MPa, the transition to two-phase flow occurs closer to the middle of the pipe. For pressures of 14 and 13 MPa the phase transition point ranges from 3/5 to 2/3 of the length. These values fluctuate, but the general nature remains the same.

The exception in a number of experiments is a 0.8 m long pipe. In this case, the choked flow phenomenon occurs at the outlet section of the pipe and the phase transition begins there only. This can be explained by insufficient pipe length to reach the saturation parameters.

5. Conclusions

The success of the simulation showed us in detail at which point in the pipes the critical flow occurs. Recalling that the critical flow was induced to be analyzed, the simulations showed that in most cases, many cells showed its occurrence most of the time at the end of the pipe,

Void fraction graphs indicate the presence of bubbles inside the pipes, few cases had large amount of void formation as result of the critical flow phenomena and other cases no significant amount of void was formed.

One of the reasons for the simulation was to verify how fast the phenomenon happens and it was possible to verify that in some cases the number of cells had to be increased so that it was really possible to see the critical flow.

One of the things analyzed was that pipes where the primary pressure was not so different from the secondary pressure, that is, where the pressure did not decrease so much, the occurrence of critical flow was lower.

It could also be observed that longer the length of the pipe, regardless of the pressure, the more space there is, the lower the occurrence, the fluid travels the path without major changes.

In order to obtain the results, several factors that also influence the critical flow were analyzed and evaluate including the right type of material used, introduce other pressures or even develop a practical simulation to analyze the type of bubbles that occur, such as the void behaves at the time of occurrence would lead us to have a more specific answer with greater precision.

References

[1] GUERRINI, B., PACI, S., Lessons of Nuclear Plants, Part II B, Advanced Reactors, 1999, http://www2.ing.unipi.it/dip/lezioni/impnuc/advanced.pdf (Accessed 17 January 2022).

[2] WNA [World Nuclear Association]. World Nuclear Performance Report 2018. London: WNA, 2018, https://www.world-nuclear.org/our- association/publications/world-nuclear-performance-reports/world-nuclear- performance-report-2018.aspx. (Accessed 20 February 2022)

[3] TOLMASQUIM, Mauricio, Energia Termelétrica: Gás Natural, Biomassa, Carvão, Nuclear. Rio de Janeiro: EPE, 2016. 417 p., http://www.epe.gov.br/sites-pt/publicacoes-dados-abertos/publicacoes/Publicacoes Arquivos/publicacao-173/Energia%20Termel%C3%A9trica%20-%20Online%2013 maio2016.pdf. (Accessed 05 April 2022)

[4] NRC [United States Nuclear Regulatory Commission] Reactor Concepts Manual: Pressurized Water Reactor Systems.Washington: USNRC., https://www.nrc.gov/reading-rm/basic-ref/students/for-educators/04.pdf. (Accessed 22 April 2022)

[5] TVO [Teollisuuden Voima Oyj]. Nuclear Power Plant Unit Olkiluoto 3. [Eurajoki]: TVO, 2010. 64 p., https://www.tvo.fi/uploads/julkaisut/tiedostot/ydinvoimalayks_OL3_ENG.pdf . (Accessed 22 April 2022)

[6] D. T. Ingersoll, C. Colbert, R. Bromm,Z. Houghtona, NuScale Energy Supply for Oil Recovery and Refining Applications, https://international.anl.gov/training/materials/BL/NuScale-Oil-Refining-ICAPP14.pdf .(Accessed 1 February 2022)

[7] direns.mines-paristech.fr 2022. Pressurized Water nuclear power plants (online) https://direns.mines-paristech.fr/Sites/Thopt/en/co/centrales-nucleaires-eau.html. (Accessed 20 April 2022)

[8] NUSCALE POWER. Technology Validation and industry expertise. Portland, OR. US. https://www.nuscalepower.com/technology/ technology-validation . (Accessed 09 March 2022)

[9] NRC [United States Nuclear Regulatory Commission] Backgrounder on Nuclear power Plant Licensing Process Washington: NRC 2018., https://www.nrc.gov/docs/ML0521/ML052170295.pdf (Accessed 22 April 2022)

[10] IAEA [International Atomic Energy Agency]. EPR. Advanced Reactor Information System, ARIS. IAEA, Vienna, 2011a., https://aris.iaea.org/ PDF/EPR.pdf . (Accessed 15 May 2022)

[11] GLAVA 1, Reactor Construction for VVER-1000, https://studfile.net/preview/14807810/page:2/ (Accessed February 2022)

[12] CHRISTENSEN, P. C., Description of a Model of a U-Tube Steam Generator, Eletronics Department, Danish Atomic Energy Comission, Research Establishment Riso, 1972.

[13] 0AK RIDGENATIONALLABORATORYandBURNSandROE,INCOR- PORATED, Design Guide for Heat Transfer Equipment in Water- Cooled Nuclear Reactor Systems, 1975.

[14] EL-WAKIL,M.M.-NuclearEnergyConversion. Intext Educational Publishers, 1971.

[15] ELETRONUCLEAR [Eletrobras Eletronuclear]. Security Aspects of CNAA Plants Presentation done in the Internacional Conference of Nuclear Energy,2011., http://www.faap.br/cees/energianuclear/pdf/Paulo%20Christiano%20 de%20Rodrigues%20Vieira.pdf. (Accessed 10 January 2022)

[16] INSAG [International Nuclear Safety Group]. The Interface Between Safety and Security at Nuclear Power Plants. INSAG-24, IAEA, Vienna (2010)., https://www.iaea.org/publications/8457/the-interface-between-safety-and-security-at-nuclear-power-plants . (Accessed 9 May 2022)

[17] NASA Goddard Space Flight Center. Coal and gas are far more harmful than nuclear power. US, 2013, https://climate.nasa.gov/ news/903/coal-and-gas-are-far-more-harmful-than-nuclear-power/ . (Accessed 19 May 2022)

[18] IAEA [International Atomic Energy Agency]. The Fukushima Daiichi Accident. IAEA, Vienna. 2015., https://www.iaea.org/publications/ 10962/the-fukushima- daiichi-accident . (Accessed 15 December 2021)

[19] United States Nuclear Regulatory Commission, n.d. Volume 2: Modeling Guidelines. TRACE V5.0 USER'S MANUAL, (online) Washington: U. S. Nuclear Regulatory Commission. Available at: https://www.nrc.gov/docs/ML0717/ML071720510.pdf (Accessed 27 November 2022).

[20] NRC: Package ML120060403 - Final - TRACE V5.0 Manuals., https://www.nrc.gov/docs/ML1200/ML120060218.pdf (Accessed 12 July 2022)

[21] MEGEVAND, Ariel. Bubble nucleation and growth in slow cosmological phase transitions. https://www.sciencedirect.com/science/article/pii/S0550321318300129. (Accessed 20 June 2022)

[22] nuclear-power.com. 2022. Void Fraction – Two-phase Flow., https://www.nuclear-power.com/nuclear-engineering/fluid-dynamics/two-phase-fluid-flow/void-fraction-two-phase-flow/ .(Accessed 20 May 2022)